Diagnostica, Stamford, CT). The exposure of aminophospholipids on the outer leaflet of the PLT membrane was also quantified with annexin V, a placental-derived protein that also binds to the anionic phospholipids. The binding of Fg and VWF was detected with the corresponding polyclonal antibodies (Dako A/S, Denmark) previously conjugated with FITC according to standard procedures. Nonspecific membrane immunofluorescence was determined by use of the corresponding isotype of immunoglobulin-FITC and immunoglobulin-PE.

Flow cytometry analysis. Immunolabeling of PLTs with antibodies was performed with dual-color analysis. Briefly, after collection, 2.5-µL aliquots of PC were added to polypropylene tubes loaded with 50 µL of phosphate-buffered saline (PBS). Samples were first incubated with saturating concentrations of anti-CD41a-PE in the dark, without stirring, for 15 minutes at room temperature, followed by the addition of FITC-conjugated antibodies and another incubation for 15 minutes. Samples were then diluted with 1 mL of PBS and analyzed.

Blood samples were analyzed with a flow cytometer (FACScan, Becton-Dickinson, Mountain View, CA) at an excitation wavelength of 488 nm. Fluorescence and scatter signals were calibrated with 2-µm Calibrate beads (Becton-Dickinson). FITC and PE fluorescence was detected with a 530/30- and 575/26-nm bandpass filter, respectively, and overlap in the emission spectra of FITC and PE was corrected. Blood samples were diluted so that the flow rate through the laser beam was less than 3000 events per second. PLTs were differentiated from red cells and white cells (WBCs) by their specific membrane immunofluorescence. Histograms composed from fluorescence data were obtained in the logarithmic mode with 5000 cells analyzed in each sample. Mean fluorescence intensities corresponding to antibody binding (GPIbα, GPIIb-IIIa, and GPIV) were calculated with the computer software (LYSYS II 1.1 conversion software, Becton Dickinson) in an arithmetic mode on a personal computer (H-P 217, Hewlett-Packard, Palo Alto, CA). For study of CD62P, CD63, VWF, Fg, and FVa, the results were expressed as the percentage of positive PLTs for these antibodies; an analytical marker was set in the green fluorescence channel to define 2 percent of the PLT population with the highest membrane fluorescence at the baseline level. This marker was used as a threshold to determine the proportion of PLTs exhibiting immunofluorescence above this level in all subsequent samples. Procedures for flow cytometry methods have been published elsewhere.[16,17]

Perfusion studies

Preparation of perfusates. Blood for perfusions was obtained from healthy volunteers who had not taken drugs affecting PLTs in the preceding 10 days. The blood was anticoagulated with citrate-phosphate-dextrose (final citrate concentration, 19 mmol/L). PLT and WBC depletion was performed by filtration through a filter (RC100 KLE, Pall Newquay, Cornwall, UK).[18] Samples taken from the PC on different days were incorporated into thrombocytopenic blood at volumes aimed to increase the PLT count in the perfusate to 150×10^9 per L with a final volume of 20 mL. To avoid hemodilution in blood samples, hematocrit was adjusted to obtain values above 37 percent.

Perfusion experiments. Perfusions were carried out at 37°C in annular chambers according to Baumgartner.[19] Enzymatically denuded New Zealand rabbit aorta segments were mounted inverted on the central plastic rod of the perfusion chamber. Blood was recirculated through the chamber for 10 minutes at a shear rate of 800 per second with a peristaltic pump (Renal Systems, Minneapolis, MN). At the end of each perfusion, the arterial segments were rinsed with 20 mL of PBS (pH 7.2), removed from the rod, and fixed with the same buffer containing 2.5 percent glutaraldehyde. The fixed segments were histologically processed as previously described.[20]

PLTs interacting with subendothelium were evaluated according to methods described elsewhere.[21] Briefly, PLTs or groups of PLTs were classified as: contact (C), PLTs attached but not spread on the subendothelium; adhesion (A), PLTs that had spread on the subendothelium surface including small aggregates of less than 5 µm in height; and thrombi (T), PLT aggregates of more than 5 µm in height. The results are expressed as percentages of the surface of the vessel examined. The percentage of the total covered surface was obtained by adding %C + %A + %T.

Statistical analysis

Data are expressed as mean ± SEM, except were expressly indicated values. Statistical evaluation of differences among groups of studies was performed with a t test. A p value of not greater than 0.05 was considered significant.

RESULTS

Evolution of PLT counts

This study includes data from at least eight different healthy donors. PLT counts performed on nonilluminated (UN-I) concentrates remained in the initial range throughout the storage period. Illumination of PCs resulted in a very mild decrease in PLT counts (Table 1).

Biochemical characterization of PLTs by flow cytometry analysis

Presence of major PLT glycoproteins and adhesive ligands. Flow cytometry studies indicated that the presence of GPIbα remained stable during the storage on UN-

I PLTs (Fig. 1). Significant reductions of this glycoprotein were observed in concentrates exposed to PRT at 12.3 J per mL, but not at 6.2 J per mL, on Day 5 of storage. Modifications in GPIIb-IIIa or GPIV levels along storage did not reach values of significance when PCs had been exposed to PRT treatment at either dose level (Fig. 1). Binding of VWF and Fg to PLTs was not significantly modified either by illumination treatment (PRT 6.2 and PRT 12.3) nor by storage conditions (0, 3, and 5 days; Fig. 2).

Interestingly, levels of fibronectin seemed to be more elevated when PLTs were exposed to PRT 12.3 ($p \leq 0.05$), but not in samples treated with 6.2 J per mL. The normal level tended to be restored toward the end of the storage interval.

Expression of activation-dependent antigens. Flow cytometry studies revealed a progressive and significant increase in the main PLT activation markers (P-selectin and LIMP) during storage ($p \leq 0.05$). A similar pattern of increase was also observed in PCs not subjected to illumination (UN-I). Exposure of concentrates to PRT 6.2 or PRT 12.3 was associated with an increase in percentages of PLTs expressing these activation markers (Fig. 3). Levels of P-selectin and LIMP found in studies with 6.2 J per mL were consistently below those observed with the higher illumination intensities, suggesting a pattern of UV dose-dependent activation marker expressions.

Apoptosis and expression of procoagulant activities. UN-I PLTs maintained similar annexin V binding levels during the storage. No significant differences were observed. A significant increase in annexin V binding was detected when flow cytometric procedures were applied to PLTs from concentrates that had been exposed to 12.3 J per mL, but not for samples treated with 6.2 J per mL (Fig. 4).

The presence of FVa on the surface of UN-I and illuminated PLTs significantly increased during storage. Although more elevated levels of FVa were observed on PRT-treated samples, no significant differences could be found between treated and untreated groups (Fig. 4).

TABLE 1. Modification of PLT counts along the storage time

	PLT count ($\times 10^3/\mu L$)		
Variable	Day 0	Day 3	Day 5
UN-I	1345 ± 35	1349 ± 41	1378 ± 47
PRT 6.2	1206 ± 32*	1143 ± 36*	1172 ± 43*
UN-I	1012 ± 19	1026 ± 29	1008 ± 32
PRT 12.3	1012 ± 20	949 ± 31*	922 ± 34*

* $p < 0.05$ vs. UN-I samples.

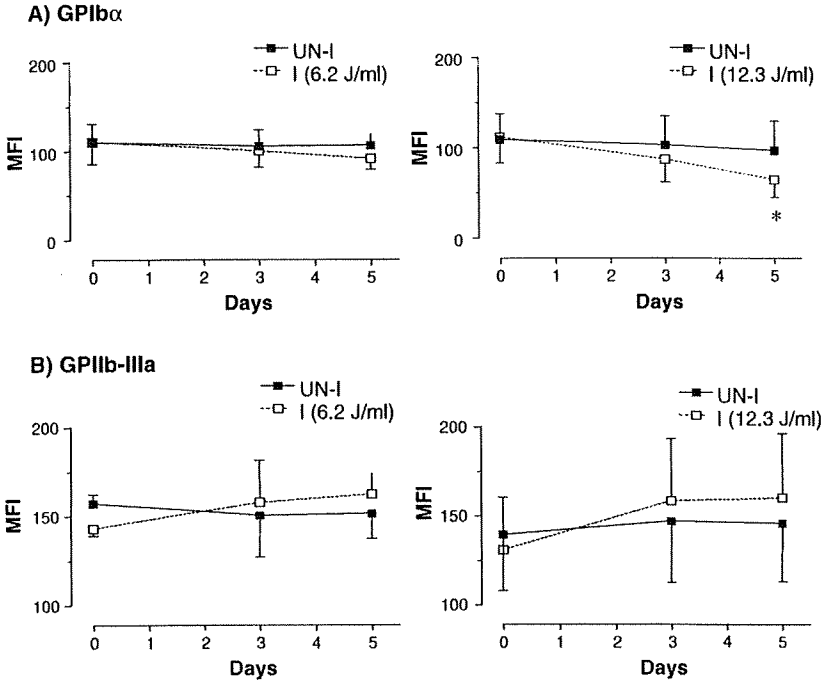

Fig. 1. Flow cytometry studies of presence of GPIbα (A) and GPIIb-IIIa (B) on nonilluminated (UN-I, ■) PLTs and illuminated (I, □) PLTs with 6.2 (left) and 12.3 (right) J per mL for 5 days of storage (mean ± SD, n = 8, *$p < 0.05$).

Evaluation of adhesive and aggregating activities in perfusion systems with circulating blood

Perfusion studies performed with UN-I PLTs on Day 0 resulted in a PLT coverage equivalent to 25.7 ± 1.7 percent of the perfused subendothelial surface (mean ± SEM, n = 8). Similar studies with PLTs exposed to 6.2 J per mL (illuminated) resulted in a mild decrease of the surface covered by PLTs (5.19 ± 2.2%, $p < 0.05$) (Fig. 5A). PLT storage did not modify PLT deposition, in either treated (illuminated) or nontreated (UN-I) samples. Exposure of PLTs to PRT 6.2 did not have a deleterious effect on PLT functions. In fact, a slight increase in PLT reactivity toward the subendothelium was observed on Day 5 of storage when compared to values of the respective nontreated concentrates (Fig. 5). In contrast, exposure of PCs to more elevated illumination intensities caused alterations in the abilities of PLTs to interact with the subendothelium. The alterations observed seemed to follow a light dose-dependent relationship. Reductions of adhesive and aggregating capacities of PLTs were noted in PCs exposed to PRT 12.3 on Day 5

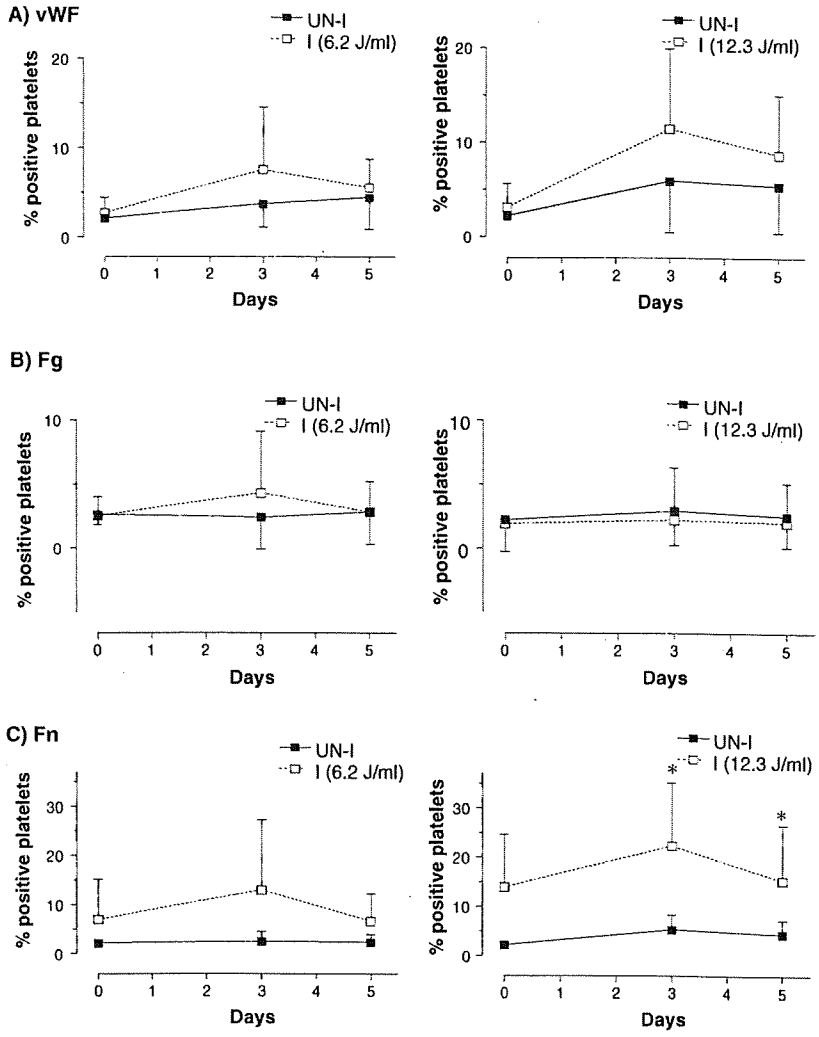

Fig. 2. Results of flow cytometry studies showing the binding of VWF (A), Fg (B), and fibronectin (C) on nonilluminated (UN-I, ■) and illuminated (I, □) PLTs with 6.2 (left) and 12.3 (right) J per mL for 5 days of storage (mean ± SD, n = 8, *p < 0.05).

(Fig. 5B). An exhaustive analysis of the different interaction classes (%C, %A, and %T) is provided in Fig. 5.

DISCUSSION

Inactivation of pathogens in blood products with photochemical procedures is a promising strategy to improve blood safety. Current strategies for pathogen reduction in blood products, however, could have a deleterious effect on PLT integrity and functions. In this study, we have evaluated the impact of a new technology for pathogen reduction based on riboflavin and UV light exposure on functional characteristics of PCs. Flow cytometry studies revealed changes in antigens and activation indicators that were compatible with those observed in standard PCs used routinely for transfusion. Functional studies in perfusion models confirmed that PLTs in PCs treated with the low energy (6.2 J/mL) preserved adhesive and cohesive function to levels compatible with those observed in the respective nontreated controls. Overall our data indicate that PLT function was well preserved in PCs treated with this new technology with the energy of 6.2 J per mL.

Riboflavin is a naturally occurring compound and essential human nutrient. Previous studies indicated that this nutrient could be effective for pathogen reduction when exposed to visible or UV light, suggesting that riboflavin could act as a useful photosensitizer for the inactivation of pathogens. Recent studies have confirmed that the pathogen reduction strategy of riboflavin plus UV light (Mirasol PRT) was effective in reducing bacterial and viral contamination in PCs.[13,22] Having confirmed the efficacy of the procedure for pathogen inactivation, the major question remaining is whether this PRT could affect functional aspects of the treated PCs. This study has focused on the functional aspects of PLTs exposed to the riboflavin plus UV PRT.

PLT storage lesions have been demonstrated in PCs collected by different procedures as PLT-rich plasma, buffy coat (BC), and apheresis and seem to develop very early during the preparation of PCs.[10,11] The extent of activation and the subsequent deterioration upon storage, however, differs significantly depending on separation procedures. Comparative studies with flow cytometry techniques indicate, in general, that PLTs collected by the PLT-rich plasma method showed greater alterations, apheresis procedures could induce moderate changes, and PCs procured from BC show lesser activation.[9-11,23-25]

Alterations in PLTs harvested through apheresis procedures seem to depend highly on cell separator technology. Modifications in shear stress, biocompatibility of surfaces, and recollection of the PLTs may result in variable degrees of PLT activation and thereby affect the quality of the component. In these studies, the Trima Accel of Gambro BCT was used for PLT separation.. Interestingly, PLTs collected by this cell separator showed levels of activation markers such as P-selectin in a range similar to those found in PLTs obtained by the BC method[10,11,26] and in any case comparable to those of

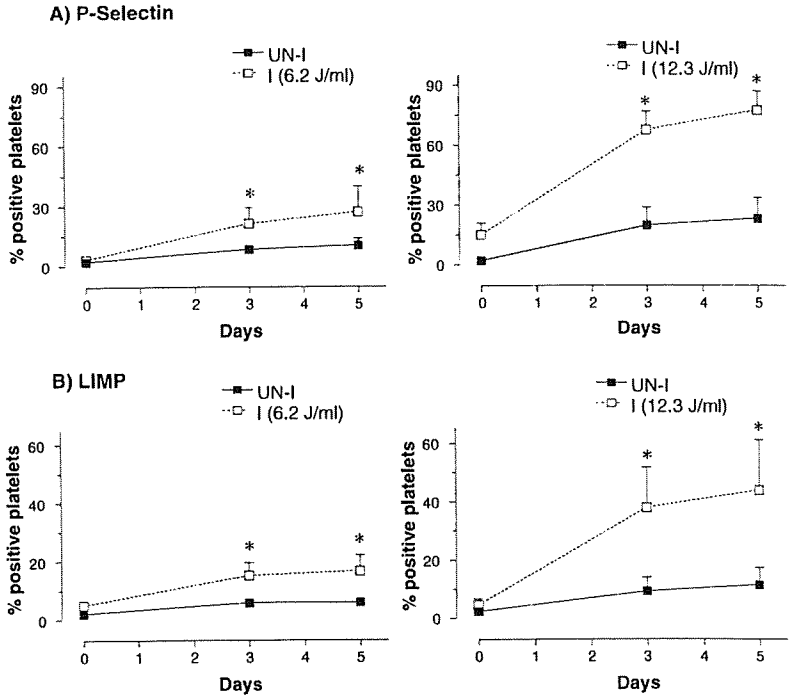

Fig. 3. Graphs showing percentage of PLTs positive for P-selectin (A) and LIMP (B) measured by flow cytometry on nonilluminated (UN-I, ■) and illuminated (I, □) PLTs with 6.2 (left) and 12.3 (right) J per mL for 5 days of storage (mean ± SD, n = 8 *p < 0.05).

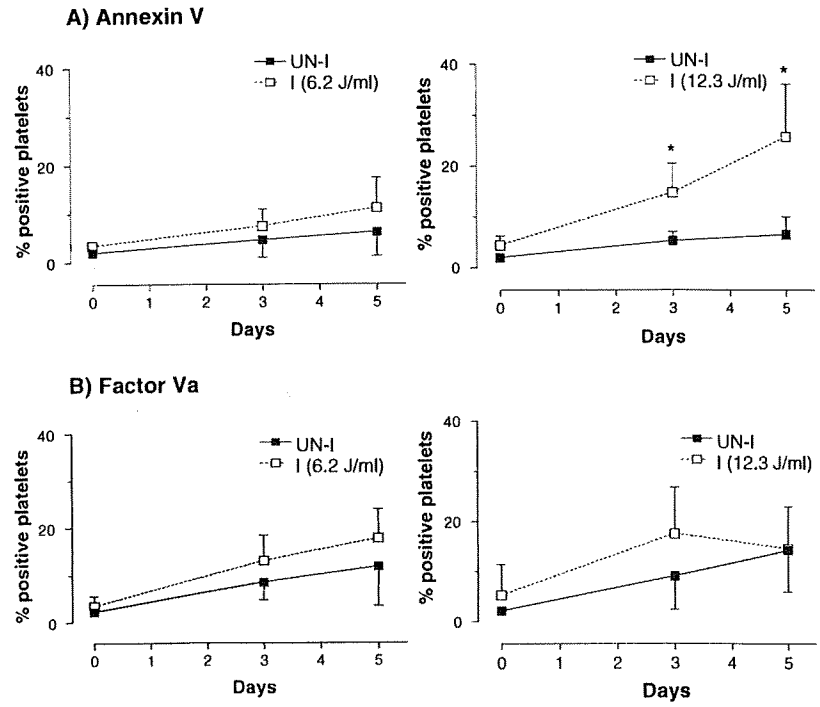

Fig. 4. Graphs showing procoagulant activity measured by annexin V binding (A) and FVa (B) binding on nonilluminated (UN-I, ■) PLTs and illuminated (I, □) PLTs with 6.2 (left) and 12.3 (right) J per mL for 5 days of storage (mean ± SD, n = 8, *p < 0.05).

other cell separators with technical improvements to reduce PLT activation.[24]

In this study, exposure of PCs to Mirasol PRT treatment caused a very mild decrease in PLT counts. Similar reductions have been reported with other PRT technologies.[27] The Mirasol technology used in our studies seemed to have a minimal impact on major PLT glycoproteins. Analysis of our flow cytometry data showed a steady presence of major membrane GPs, GPIbα and GPIIb-IIIa, perfectly compatible with observations from other studies with BC PLTs[10,11] or with PLTs separated by apheresis procedures.[24] PLT activation markers (P-selectin and LIMP) showed a tendency to increase along storage in both the control and the Mirasol-treated groups. This tendency was more evident in PCs that had been exposed to the highest energy (12.3 J/mL). Observations of these studies are comparable to those reported for other photochemical inactivation procedures.[26,28] Under our experimental conditions, the PRT procedure also increased the binding of ligands such as fibronectin, or VWF, but not Fg, whose levels were very similar in treated and nontreated PCs and consistently stable during the 5-day storage period.

Careful attention was paid to modifications of annexin V binding to PLTs stored as concentrates. Annexin V binds to negatively charged phospholipids.[29,30] In nucleated cells, an enhanced binding of annexin V is an indicator of apoptosis.[31] Loss of membrane asymmetry and a subsequent binding of annexin V is observed in PLTs exposed to strong activators.[32,33] An excessive binding of annexin V can also be observed in PLTs that have become "apoptotic" because of prolonged conservation.[34] In our study, an increase of binding of annexin V was found in PLTs that had been exposed to the higher illumination energies. Interestingly, exposure of PCs to 6.2 J per mL resulted in very moderate exposure of negatively charged phospholipids. These would indicate the existence of a threshold in illumination energies from 6.2 to 12.3 J

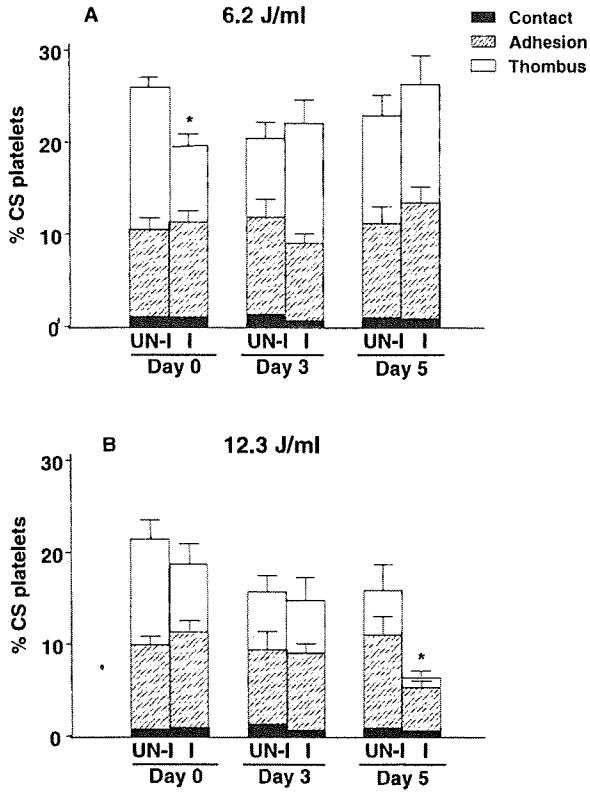

Fig. 5. Bar diagrams showing the percentage of coverage surface (CS) by PLTs classified in percentage of contact (filled bars), adhesion (dashed bars), and thrombi formation (open bars), performed by nonilluminated PLTs (UN-I) and illuminated PLTs (I) at 6.2 (A) and 12.3 J per mL (B) for 5 days storage (mean ± SEM, n = 8, *p < 0.05 vs. UN-I).

per mL that may have a critical impact on PLT quiescence. Nevertheless, studies from our group have demonstrated that loss of adhesive and aggregating properties in PLTs subjected to prolonged storage might be partially compensated by the development of procoagulant activity.[35,36] Interestingly, this procoagulant activity is the direct result of the exposure of negatively charged phospholipids and revealed by an increased annexin V binding to the PLTs or their derived microparticles.

Perfusion models have been successfully used for the assessment of mechanisms of action of blood components and for the evaluation of the dynamic and shear-induced PLT functionality in circulating blood. These techniques have been applied to fill the gap between experimental and clinical investigations in transfusion medicine.[36] Only a few studies have been published in relation to the effect of separation methods or storage on PLTs, however.[11,37,38] Our group has developed extensive experience in the evaluation of in vitro hemostatic effectiveness of PCs in perfusion models.[11,35,36,39,40] In this study, we have found that illumination of PLTs at 6.2 J per mL was followed by a milder deterioration on their adhesive and aggregating functions when results were compared with higher illumination equivalent to 12.3 J per mL, where PLT interaction was decreased.

The results on Day 5 in PCs treated with 6.2 J per mL are in favorable contrast with previous experience from our group. We have previously communicated that adhesive and cohesive functions of PLTs tend to decrease with storage time.[35] Although results from perfusion experiments with PCs exposed to higher levels of energy showed a progressive reduction in adhesive and cohesive functions of PLTs on the 5th day, those from PCs treated with 6.2 J per mL did not show such a decay. We hypothesize that specific conditions produced during the PRT at low energy might delay the deleterious effect of storage that we have consistently observed with other PCs. In any case, if as we postulate, results from perfusion studies can be extrapolated to the clinical outcome, modifications observed with energies equivalent to 6.2 J per mL should not have significance for the transfusion practice.

In summary, our studies in dynamic systems with circulating blood indicate that PLT function is well preserved in concentrates exposed to low energy (6.2 J per mL) and still reasonably preserved in those that had been exposed to higher energy (12.3 J per mL). Our results combined with those from recently published studies indicate that 6.2 J per mL would preserve a favorable compromise between pathogen reduction and functional capacities in the exposed PCs. Ultimately, controlled clinical trials should answer to what extent the experimental observations provided by this study will translate into transfusion efficiency in the clinical thrombocytopenic patient.

ACKNOWLEDGMENTS

The authors thank Montserrat Viñas, Marc Pino, and Marta Palomo for the excellent technical assistance and Montse Riego for secretarial help.

REFERENCES

1. Sakariassen KS, Bolhuis PA, Sixma JJ. Human platelet adhesion to artery subendothelium is mediated by factor VIII-von Willebrand factor bound to the subendothelium. Nature 1979;279:636-8.
2. Nieuwenhuis HK, Sakariassen KS, Houdijk WP, et al. Deficiency of platelet membrane glycoprotein Ia associated with a decreased platelet adhesion to subendothelium: a defect in platelet spreading. Blood 1986;68:692-5.
3. Kehrel B, Wierwille S, Clemetson KJ, et al. Glycoprotein VI is a major collagen receptor for platelet activation: it recognizes the platelet-activating quaternary structure of collagen, whereas CD36, glycoprotein IIb/IIIa, and von Willebrand factor do not. Blood 1998;91:491-9.

4. Sakariassen KS, Nievelstein PF, Coller BS, et al. The role of platelet membrane glycoproteins Ib and IIb-IIIa in platelet adherence to human artery subendothelium. Br J Haematol 1986;63:681-91.
5. Ruggeri ZM, Dent JA, Saldivar E. Contribution of distinct adhesive interactions to platelet aggregation in flowing blood. Blood 1999;94:172-8.
6. Bevers EM, Comfurius P, Zwaal RF. Platelet procoagulant activity: phyisiological significance and mechanims of exposure. Blood Rev 1991;5:146-54.
7. Weiss HJ, Hoffmann T, Turitto VT, et al. Further studies on the presence of functional tissue factor activity on the subendothelium of normal human and rabbit arteries. Thromb Res 1994;73:313-26.
8. Hoffman M, Monroe DM, Roberts HR. Activated factor VII activates factors IX and X on the surface of activated platelets: thoughts on the mechanism of action of high-dose activated factor VII. Blood Coagul Fibrinolysis 1998;9:S61-S65.
9. Bessos H, Atkinson A, McGill A, et al. Apheresis platelet concentrates: correlation of day one levels of in vitro quality markers with corresponding levels on days two to five of storage. Thromb Res 1996;84:367-72.
10. Metcalfe P, Williamson LM, Reutelingsperger CP, et al. Activation during preparation of therapeutic platelets affects deterioration during storage: a comparative flow cytometric study of different production methods. Br J Haematol 1997;98:86-95.
11. Lozano M, Estebanell E, Cid J, et al. Platelet concentrates prepared and stored under currently optimal conditions: minor impact on platelet adhesive and cohesive functions after storage. Transfusion 1999;39:951-9.
12. Estebanell E, Diaz-Ricart M, Escolar G. Alterations in cytoskeletal organizatrion and tyrosine phosphorylation in PCs prepared by the BC method. Transfusion 2000;40:535-42.
13. Ruane PH, Edrich R, Gampp D, et al. Photochemical inactivation of selected viruses and bacteria in platelet concentrates using riboflavin and light. Transfusion 2004;44:877-85.
14. Li J, De Korte D, Woolum MD, et al. Pathogen reduction of buffy coat platelet concentrates using riboflavin and light: comparisons with pathogen-reduction technology-treated apheresis platelet products. Vox Sang 2004;87:82-90.
15. AuBuchon JP, Herschel L, Roger J, et al. Efficacy of apheresis platelets treated with riboflavin and ultraviolet light for pathogen reduction. Transfusion 2004;44(Suppl):16.
16. Lozano M, Escolar G, White JG, et al. Redistribution of membrane glycoproteins in platelets activated under flow conditions. Blood Coagul Fibrinolysis 1996;7:214-7.
17. Escolar G, Lozano M, DiazRicart M, et al. Modifications in accessibility of membrane glycoproteins, binding of specific ligands and coagulation factor V during the activation of platelets in blood emerging from bleeding time wounds. Am J Hematol 1999;60:260-7.
18. Galan AM, Hernandez MR, Bozzo J, et al. Preparations of synthetic phospholipids promote procoagulant activity on damaged vessels: studies under flow conditions. Transfusion 1998;38:1004-10.
19. Baumgartner HR. The role of blood flow in platelet adhesion, fibrin deposition and formation of mural thrombi. Microvasc Res 1973;5:167-79.
20. Escolar G, Bastida E, Ordinas A, et al. Interaction of platelets with subendothelium in humans treated with aspirin and dipyridamole alone or in combination. Thromb Res 1985;40:419-24.
21. Escolar G, Mazzara R, Castillo R, et al. The role of the Baumgartner technique in transfusion medicine: research and clinical applications. Transfusion 1994;34:542-9.
22. Li J, De Korte D, Woolum M, et al. Performance of the Mirasol PRT system with buffy coat platelet and apheresis platelet concentrates. Vox Sang 2004;87:S17-92.
23. Eriksson L, Kristensen J, Olsson K, et al. Evaluation of platelet function using the in vitro bleeding time and corrected count increment of transfused platelets. Vox Sang 1996;70:69-75.
24. Hagberg IA, Akkok CA, Lyberg T, et al. Apheresis-induced platelet activation: comparison of three types of cell separators. Transfusion 2000;40:182-92.
25. Rinder HM, Snyder EL, Bonan JL, et al. Activation in stored platelet concentrates—correlation between membrane expression of P-selectin, glycoprotein IIb/IIIa, and beta-thromboglobulin release. Transfusion 1993;33:25-9.
26. van Rhenen D, Gulliksson H, Cazenave JP, et al. Transfusion of pooled buffy coat platelet components prepared with photochemical pathogen inactivation treatment: the euroSPRITE trial. Blood 2003;101:2426-33.
27. Janetzko K, Lin L, Eichler H, et al. Implementation of the INTERCEPT blood system for platelets into routine blood bank manufacturing procedures: evaluation of apheresis platelets. Vox Sang 2004;86:239-45.
28. Picker SM, Speer R, Gathof BS. Functional characteristics of buffy-coat PLTs photochemically treated with amotosalen-HCl for pathogen inactivation. Transfusion 2004;44:320-9.
29. Xiao HY, Matsubayashi H, Bonderman DP, et al. Generation of annexin V-positive platelets and shedding of microparticles with stimulus-dependent procoagulant activity during storage of platelets at 4°C. Transfusion 2000;40:420-7.
30. Thiagarajan P, Tait JF. Collagen-induced exposure of anionic phospholipid in platelets and platelet-derived microparticles. J Biol Chem 1991;266:24302-7.
31. van Engeland M, Nieland LJ, Ramaekers FC, Schutte B, Reutelingsperger CP. Annexin V-affinity assay: a review on an apoptosis detection system based on phosphatidylserine exposure. Cytometry 1998;31:1-9.
32. Dachary-Prigent J, Freyssinet JM, Pasquet JM, Carron JC, Nurden AT. Annexin V as a probe of aminophospholipid exposure and platelet membrane vesiculation: a flow

cytometry study showing a role for free sulfhydryl groups. Blood 1993;81:2554-65.
33. Diaz C, Schroit AJ. Role of translocases in the generation of phosphatidylserine asymetry. J Membr Biol 1996;151:1-9.
34. Li J, Xia Y, Bertino AM, et al. The mechanism of apoptosis in human platelets during storage. Transfusion 2000;40: 1320-9.
35. Hernandez MR, Bozzo J, Mazzara R, et al. Platelet concentrates promote procoagulant activity: evidence from experimental studies using a perfusion technique. Transfusion 1995;35:660-5.
36. Escolar G, Galan AM, Mazzara R, et al. Measurement of platelet interactions with subendothelial substrata: relevance to transfusion medicine. Transfus Med Rev 2001;15:144-56.
37. McGill M, Brindley DC. Effects of storage on platelet reactivity to arterial subendothelium during blood flow. J Lab Clin Med 1979;94:370-80.
38. Boomgaard MN, Gouwerok CW, Homburg CH, et al. The platelet adhesion capacity to subendothelial matrix and collagen in a flow model during storage of platelet concentrates for 7 days. Thromb Haemost 1994;72:611-6.
39. Alemany M, Hernandez MR, Bozzo J, et al. In vitro evaluation of the hemostatic effectiveness of non-viable platelet preparations: studies with frozen-thawed, sonicated or lyophilized platelets. Vox Sang 1997;73:36-42.
40. Escolar G, Mazzara R, White JG, et al. Contribution of perfusion techniques to the evaluation of the hemostatic effectiveness of platelet concentrates. Blood Cells 1992;18:403-15.

Transfusion and Apheresis Science 40 (2009) 79–85

Contents lists available at ScienceDirect

Transfusion and Apheresis Science

journal homepage: www.elsevier.com/locate/transci

Cell integrity and mitochondrial function after Mirasol-PRT treatment for pathogen reduction of apheresis-derived platelets: Results of a three-arm in vitro study

Susanne M. Picker*, Alexander Steisel, Birgit S. Gathof

Transfusion Medicine, University of Cologne, Kerpener Str. 62, 50937 Cologne, Germany

ARTICLE INFO

Keywords:
Pathogen reduction
Mirasol
Mitochondrial function
Apoptosis

ABSTRACT

Background: Mirasol pathogen reduction technology (PRT) treatment uses riboflavin (vitamin B_2) in combination with ultraviolet light (UV) to inactivate pathogens in platelet concentrates (PCs). This treatment has been reported to increase glycolytic flux, which could result from damage to mitochondria and/or increased ATP demand.
Design: Triple-dose PCs were collected by the Trima Accel™ device. Immediately after splitting, single units were designated to Mirasol-PRT treatment (M), gamma irradiation (X) or remained untreated (C). Platelet (PLT) mitochondrial transmembrane potential ($\Delta\psi$) was evaluated (JC-1 assay) as well as mitochondrial enzymatic activity (MTS assay). LDH release, p selectin expression, glucose/oxygen consumption and lactate production rates were quantified and compared among study groups during 7 days of storage.
Results: Immediately after PRT treatment, no significant changes were found in JC-1 signal, MTS activity, and LDH release indicating that PRT treatment did not alter functional/structural cell or mitochondrial integrity as evidenced by LDH release comparable to untreated study groups. In parallel to significantly higher p selectin expression, treated PLTs exhibited significantly accelerated oxygen and glucose consumption rates associated with increased acidity due to higher lactate production rates throughout storage. Despite larger cell populations with depolarized $\Delta\psi$ particularly at days 5 and 7, mitochondrial reduction activity of M units as measured by the MTS assay was maintained and appeared to be up-regulated relative to untreated and irradiated controls.
Conclusion: Mirasol-PRT treated PLTs increased both glycolytic flux as well as respiratory/enzymatic mitochondrial activity. An increased demand for ATP due to increased α granule degranulation may be the driving force for these observations.

1. Introduction

Due to advances in blood donor screening and testing, virus transmission rates have been reduced by more than 10,000-fold in the past two decades [1]. Current concerns regard missing detection in case of unrecognized or emerging agents and the "window period" during which an infected individual may be test negative but still are capable of disease transmission. Also of concern are bacterial contamination rates of blood products, especially room-temperature-stored platelets (PLTs), meanwhile recognized as one of the greatest risks for blood transfusion, directly after clerical errors [2]. Thus, important health benefits may accrue with the introduction of pathogen reduction technologies (PRT) that target nucleic acids to preclude transcription and translation of pathogens' genetic material, thereby reproduction, activation, and growing.

* Corresponding author. Tel.: +49 221 478 4868/3877; fax: +49 221 478 3155.
E-mail address: susanne.picker@uk-koeln.de (S.M. Picker).

1473-0502/$ - see front matter © 2009 Elsevier Ltd. All rights reserved.
doi:10.1016/j.transci.2009.01.013

Recently, a new PRT technology, the Mirasol™-PRT system (Navigant, Lakewood, CO, USA) using riboflavin (vitamin B_2) in combination with ultraviolet (UV) light (265–370 nm) has been shown to be effective ($\geqslant$3–6 log reduction) against a broad variety of pathogens [3–7]. As a naturally occurring essential dietary nutrient, riboflavin is considered as being non toxic [8–14].

Human PLTs, although terminally differentiated and enucleated, are not completely free of nucleic acids. Messenger RNA is detectable in the cytosol and functional proteins of the respiratory chain are coded by mitochondrial DNA. PLTs, like nucleated cells, use glucose as a major energy source for biologic energy in the form of ATP. Two metabolic pathways are responsible for ATP production: anaerobic glycolysis occurring in the PLT cytosol and aerobic oxidative phosphorylation of the glycolytic product pyruvate. The latter occurs in PLT mitochondria and is estimated to contribute approximately 80% of total ATP production in resting PLTs [15,16]. Oxidative phosphorylation is able to produce 19-fold more ATP than anaerobic glycolysis, which delivers a total net of two ATP plus two lactate molecules per metabolized glucose molecule. Previous work had indicated that UV light increases the glycolytic flux in favor of anaerobic glycolysis resulting in higher lactate levels and subsequently lower pH values [2,7,17,18], which could affect PLT viability during storage [19]. Increase in glycolytic flux could either be explained as a result of alteration in PLT ATP consumption rate or impaired mitochondria-based oxidative phosphorylation, which has to be counterbalanced by an increase in anaerobic glycolysis to maintain sufficient ATP levels. Reduced mitochondrial function could also be related to the occurrence of apoptosis [20], even in enucleated cells [16,21], which may have direct consequences for a prolonged storage of PRT treated PLTs.

For these reasons, we evaluated PLT mitochondrial integrity and enzymatic characteristics as well as metabolic status after Mirasol-PRT treatment to determine if changes in PLT metabolism were due to direct damage to PLT mitochondria or altered metabolic activity during storage.

2. Materials and methods

2.1. Preparation of PLT concentrates (PCs)

After written informed consent and passing eligibility criteria based on German blood banking requirements for PLT donation [22], a total of 12 triple-dose collections was performed using the TRIMA ACCEL™ apheresis collection device, version 5.0 (Gambro BCT, Lakewood, CO, USA). The collection targets per procedure were at least 8.5×10^{11} PLTs in at least 510 mL autologous plasma to facilitate the division of the product into three aliquots (bags). The whole collection units averaged a volume of 714 ± 13 mL and a PLT concentration of 1267 ± 117 × 10^9/L (corresponding to a mean collection dose of 9.0×10^{11}) and were kept undisturbed for two hours at ambient temperature prior to splitting and subsequent processing to allow dissociation of any PLT aggregates. All units were leukodepleted by the process-controlled leukoreduction system of the collection device. Immediately after splitting, the single units were designated to Mirasol-PRT treatment (M) or 30-Gy-gamma irradiation (X) or remained untreated (C) to serve as controls. In order to ensure the same storage conditions for all units, the 1-L ELP™ bag (extended Life Platelet, Gambro BCT) was used for storage of all three types of PCs.

2.2. Treatment with the Mirasol-PRT system

Mirasol-PRT treatment was performed on day 0 as described previously [2,23–26].

2.3. Sampling and storage of PLT concentrates

After the addition of riboflavin but before illumination, day-0 samples were taken aseptically from the illumination bag of M units, in parallel with samples taken from the other units, immediately prior to gamma irradiation (X) and storage (C). All 36 single units were then stored at 22 ± 2 °C on a flatbed agitator (Helmer Laboratories, Noblesville, IN, USA) running at 50 to 60 agitations per minute for 7 days. Additional samples were taken aseptically on storage days 1 (to examine the immediate effects of treatment), 5, and 7 (to examine longer-term effects). Day 0 was defined as the day of collection. Analyses were completed within 4 h after sampling.

2.4. Blood gas analysis and metabolic parameters

Unit pH, pO_2, pCO_2, HCO_3^-, and base excess (BE), as well as lactate and glucose contents were measured using an automated blood gas analyzer (Rapidlab 1260, Siemens Medical Solutions Diagnostics mbH, Fernwald, Germany) immediately after sampling. Unit pH, pO_2, and pCO_2 were analyzed at 37 °C and standardized to 22 °C. The overall rates for lactate production and glucose consumption (nmoL per 10^{12} cells per storage time in hours) were calculated with a total PLT count normalized to the initial PLT dose obtained on day 0 after sampling using an automated cell counting system (Sysmex K1000, Sysmex, Hamburg, Germany).

2.5. Expression of membrane bound p selectin

In resting PLTs p selectin is stored in α granules and becomes detectable on PLT surface only after PLT activation. Flow cytometric analysis of p selectin expression was performed as described recently [17].

2.6. MTS reduction assay

The MTS assay was performed as described by Li et al. [16] and the manufacturer's instructions (Promega, Madison, WI, USA). Mitochondria-based dehydrogenase enzymes of viable, metabolically active cells produce "reducing equivalents" such as NAD(P)H that convert the tetrazolium salt of the MTS assay into an aqueous, soluble formazan product quantified by the absorbance at 490 nm in a 96-well spectrophotometric plate reader (Tecan

SPECTRA, Tecan Deutschland mbH, Crailsheim, Germany). Because at death, cells rapidly lose their reduction ability, the production quantity of the formazan product is directly proportional to the number of living cells in culture.

2.7. JC-1. assay

Disruption of the PLT mitochondrial function has been shown to precede PLT apoptotic cell death [21,27,28]. Mitochondrial function can be quantitatively assessed by measuring changes in the PLT mitochondria transmembrane potential ($\Delta\psi$) using the JC-1 (J-aggregate-forming lipophilic cationic fluorochrome 5,5′,6,6′-tetrachloro-1,1′3,3′-tetraethylbenzimidazolylcarbocyanine iodide) assay (BD™ MitoScreen, BD Biosciences Pharmingen, San Diego, CA, USA). In case of polarized $\Delta\psi$ indicating healthy cells with intact oxidative phosphorylation, JC-1 is rapidly taken up into the mitochondria and forms aggregates (red fluorescence emission at 590 nm in FL2 channel). In mitochondria undergoing a transition from polarized to depolarized $\Delta\psi$ (due to altered function or apoptosis), JC-1 leaks out of the mitochondria and forms monomers in the cytoplasm (green fluorescence emission at 525 nm in FL1 channel).

The PMT values of the detectors in the FL1 and FL2 channels of the flow cytometer used (FACScan with software CELLQuest Pro, Becton Dickinson, San Jose, CA, USA) were set at 554 V and 672 V, the FL1–FL2 and FL2–FL1 compensations at 1.2% and 31.9%, respectively. The ratio of the geometric mean fluorescence intensity (MFI) between FL1 and FL2 was calculated for each sample analyzed. Calcium ionophore A 23187 (Serva Electrophoresis GmbH, Heidelberg, Germany) served as positive control in each assay due to its ability to induce $\Delta\psi$ depolarization to nearly 100%.

2.8. Statistical analysis

The results of cell quality tests are expressed as mean ± standard deviation. Statistical analysis was conducted comparing all three types of units with the Kruskal–Wallis test (SPSS 15.0 for Windows, SPSS Software GmbH, Munich, Germany). In case of significant differences ($p < 0.05$), post-hoc paired comparisons were made with the Mann–Whitney-*U*-test. Here, according to Bonferroni correction, a p value <0.017 was related to a significance level of 5%.

3. Results

Apheresis procedures were well tolerated by all study subjects. All units' bacterial cultures were negative after 16-days of incubation under aerobic and anaerobic conditions, respectively.

3.1. Contamination with rest cells, PLT count, LDH release, p selectin expression

Contaminating white blood cells, red blood cells and citrate averaged mean values of $0.46 \pm 0.47 \times 10^6$/unit, $0.81 \pm 0.17 \times 10^9$/unit, and 0.68 ± 0.02 mmoL/unit, respectively. Units' volume and PLT dose ranged from 228.7 mL to 245.9 mL and from $2.3 \times 10^{11}$to 3.6×10^{11}, respectively without proving statistical significance between study groups. Immediately after PRT treatment, no significant changes neither for PLT dose nor for LDH release were observed compared to untreated or irradiated units (Table 1), which remained consistent until the end of storage (M: 152 ± 15 U/L, C: 165 ± 31 U/L, X: 162 ± 21 U/L). The percentage of PLTs expressing p selectin on their surface increased progressively throughout storage in all types of units, significantly more pronounced after PRT treatment.

3.2. Mitochondrial function and integrity

The results of the MTS and JC-1 assay suggest, that after PRT treatment, PLTs maintain mitochondrial enzymatic activity and structural integrity at the same level as those observed in untreated and irradiated controls with the exception of larger cell populations with depolarized $\Delta\psi$ on day 1 (Table 1). During storage, C and X units maintained their initial values for $\Delta\psi$, while M units demonstrated an 8% decrease in cell populations with polarized $\Delta\psi$ and a 5-fold increase in cell populations with depolarized $\Delta\psi$ (Fig. 1). Analysis of MFI ratios suggests that for *all* types of units $\Delta\psi$ decreased by approximately 50% during 7 days of storage. This may indicate storage-related reduction of mitochondrial integrity in all units, however significantly more pronounced in M units relative to controls (C, X) by the end of storage. In contrast to C and X

Table 1
Immediate effects of Mirasol-PRT treatment on mitochondrial function and integrity.

Parameter	M = Mirasol-PRT treated (n = 12)		C = Untreated controls (n = 12)		X = Gamma irradiated (n = 12)	
	Day 0	Day 1	Day 0	Day 1	Day 0	Day 1
PLT count (×10⁹/L)	2.84 ± 0.32	2.48 ± 0.35	2.95 ± 0.32	2.69 ± 0.28	2.97 ± 0.35	2.74 ± 0.29
pH at 22 °C	7.33 ± 0.07[a,b]	7.41 ± 0.06[a,b]	7.25 ± 0.05[c]	7.52 ± 0.06[c]	7.25 ± 0.10[c]	7.53 ± 0.06[c]
Mitochondria membrane						
Polarization (%)	96.6 ± 1.8	95.5 ± 2.7	96.5 ± 2.3	97.4 ± 1.3	96.6 ± 2.0	97.3 ± 1.4
Depolarization (%)	1.83 ± 1.63	1.43 ± 0.44[a,b]	2.22 ± 2.19	0.80 ± 0.20[c]	2.00 ± 1.69	1.01 ± 0.31[c]
MTS reduction activity (OD490)	0.865 ± 0.195	0.936 ± 0.152	0.854 ± 0.141	0.819 ± 0.131	0.869 ± 0.148	0.889 ± 0.108
LDH release (U/L)	106.1 ± 12.0[a,b]	104.3 ± 13.8[a,b]	122.3 ± 16.1[c]	124.5 ± 14.7[c]	126.7 ± 9.4[c]	130.8 ± 12.1[c]
P selectin expression (%)	28.5 ± 15.3	38.4 ± 13.8[a,b]	16.8 ± 5.1	15.6 ± 7.8[c]	17.0 ± 6.5	16.0 ± 7.9[c]

Significant compared to.
[a] Untreated units (C).
[b] Gamma irradiated units (X).
[c] PRT treated units (M).

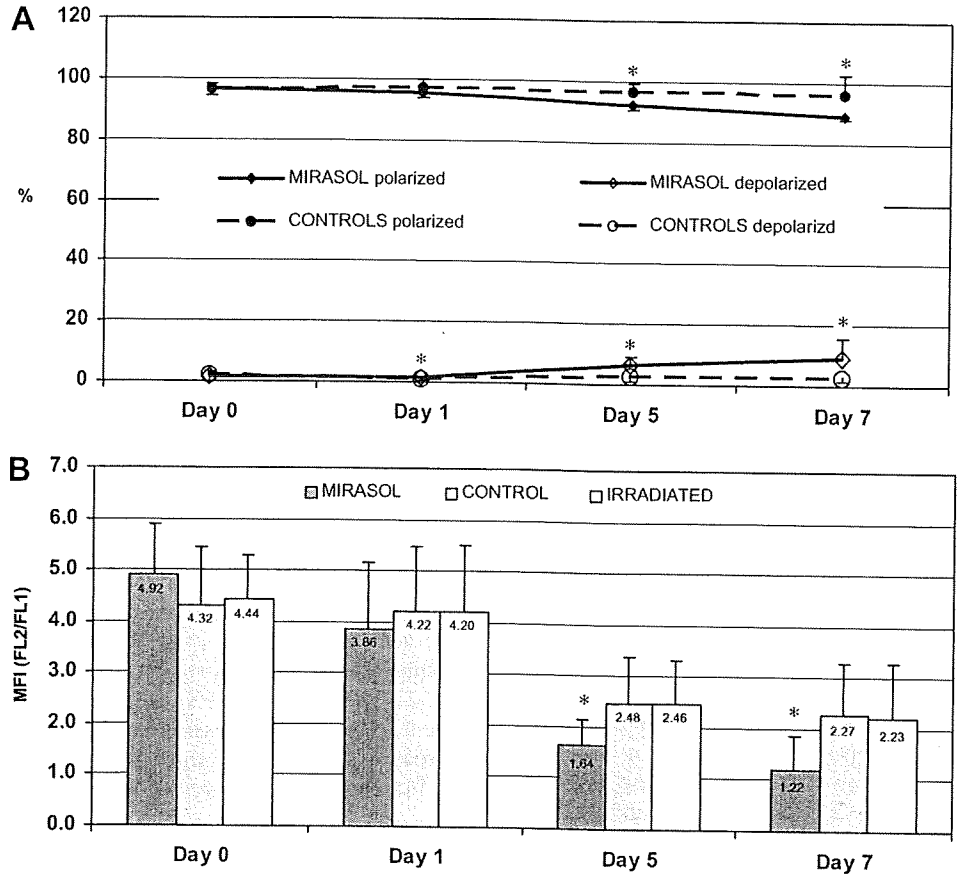

Fig. 1. Measurement of mitochondrial membrane potential by JC-1 staining assay. (A) Subpopulation percentages for PLTs with polarized and depolarized mitochondrial membranes were calculated. Untreated and irradiated units were summarized as CONTROLS. (B) The ratio of mean fluorescence intensity (MFI) between FL2 and FL1 was calculated. The JC-1 signal decreased in all types of units, more pronounced after PRT treatment. Significant differences ($^*p < 0.001$) could be found between treated and control units by storage day 5.

units (maintaining initial values), M units exhibited a 12% increase in mitochondrial reduction activity at the end of storage relative to day 0 (Fig. 2). Thus, the results of the MTS assay suggest that, regardless of $\Delta\psi$ depolarization, the mitochondrial enzymatic activity was ongoing, even up-regulated after PRT treatment.

3.3. Metabolic parameters and blood gas analysis

M units demonstrated a significantly higher rate in glucose consumption and lactate production relative to controls (C, X) associated with a significantly more pronounced decrease in sample pH (and subsequent lower levels of bicarbonate and BE). Blood gas analysis showed a storage-related increase in pO_2 and decrease in pCO_2 in all units. Applying the formula of Kilkson [29], lower pO_2 levels of M units indicated increased oxygen consumption yielding significant differences to the counterparts (C, X) until day 5 of storage (Table 2). Thus, apart from acceleration in anaerobic glycolysis, there was also an accelerated oxidative glucose metabolism performed in M units.

4. Discussion

During storage, PRT treated [7,17,30,31] or UV stressed [23,32] PLTs have the capacity to undergo apoptosis [16] and lose their functionality and structural integrity as measured by reduced in vitro aggregation, loss of membrane transport capacity, release of LDH, and morphologic changes summarized as the "PLT storage defect (PSD)" [33,34] that may contribute to transfusion reactions [35]. The molecular basis underlying and regulating these events is unknown. This is especially true for the relationship between the PSD and the programmed cell death (apoptosis). Both, the apoptotic process and the PSD lead to PLT activation and microvesiculation with enhanced phosphatidylserine (PS) expression, thus PLT-dependent thrombin-generating capacity [36,37]. Inadequate metabolic support or the accumulation of bioactive substances such as cytokines can trigger caspase-mediated cell apoptosis through an extracellular signaling pathway and have been reported to contribute to PSD, suggesting that PSD and apoptosis may be related to each other [37,38]. Meanwhile, there is an abundance of data suggesting that mitochondria play a critical role in apoptosis by releasing cytochrome c and other proteins required for the activation of the caspase signaling system. These observations led us to investigate, whether Mirasol-PRT treatment could affect mitochondrial function or energy metabolism/demand, thus increase PSD.

Overall, the results of this study suggest that Mirasol-PRT treatment did not induce significant cell lysis and that

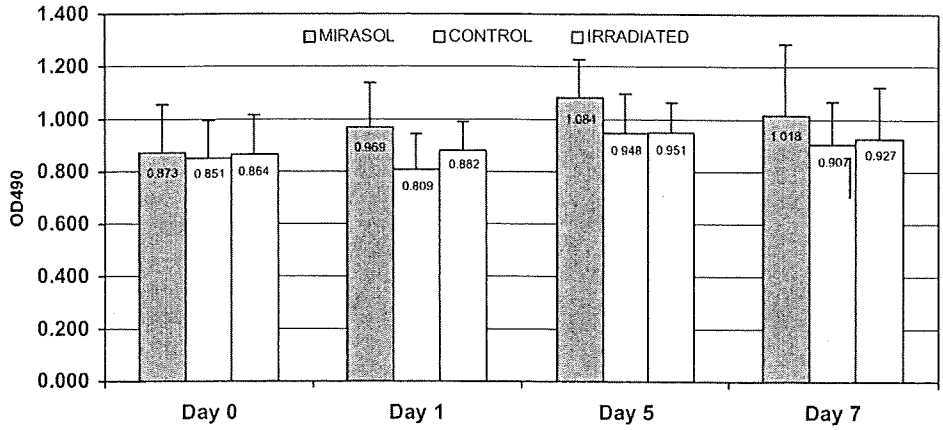

Fig. 2. Assessment of mitochondrial enzymatic activity by the MTS reduction assay. The OD readout at 490 nm was normalized to the concentration of each tested aliquot. Higher values after PRT treatment were observed relative to controls without proving statistical significance among study groups.

mitochondria of PRT treated PLTs retained functional integrity despite increased transmembrane depolarization. Apart from acceleration of PLT activation and glycolytic flux, Mirasol-PRT treatment appeared to result in an up-regulation of mitochondrial function, especially in terms of respiratory activity. Nevertheless, relative to untreated and irradiated controls, PRT treated PLTs demonstrated an increased PSD and failed with acceptance criteria for glucose consumption rate ($\leqslant$0.50 mmol/10^{12} cells/h) and pH at 22 °C ($\geqslant$6.85) at storage day 7, while lactate production rate remained acceptable ($\leqslant$0.110 mmol/10^{12} cells/h) until the end of storage.

The mitochondrial $\Delta\psi$ is indicative for oxidative mitochondria-based ATP generation. Energy released during the oxidation reactions in the mitochondrial respiratory chain is stored as a negative electrochemical gradient across the mitochondrial membrane and the $\Delta\psi$ is referred to as being polarized. Collapse of the $\Delta\psi$ results in a depolarized $\Delta\psi$ indicative either for a loss of mitochondrial integrity or a disequilibrium of the prevailing ATP/ADP ratio. Depolarization of the $\Delta\psi$ is often one of the first events occurring early during apoptosis and may even be prerequisite for cytochrome c release. Expressed as MFI ratio of FL2 over FL1, to include partially depolarized PLTs, lower values occurred by the end of storage in all units, particularly after PRT treatment. Unlike us, Li et al. [24] were not able to detect any significant differences of the $\Delta\psi$ between treated and untreated units throughout storage. Data discrepancies may be due to variable flow cytometer settings and variations of the FL2 signal based on intercellular heterogeneity within a cell population. For untreated control PLTs at day 1, Li et al. [24] reported a range in FL2 fluorescence intensity from 205 to 701 (mean 423 ± 129), while our FL2 values ranged from 228 to 417 (mean: 335 ± 64).

As reported previously [16,24], MTS reduction activity remained stable for both, treated and untreated counterparts during 7 days of storage. Moreover, MTS reduction activity seemed to be slightly elevated after PRT treatment. Given the fact that MTS activity is related to mitochondria-based dehydrogenase activity [39], PRT treatment did not affect mitochondrial function in this regard. Moreover, as seen from the lower pO_2 levels of M units, oxygen consumption was elevated after PRT treatment relative to untreated controls. Together with lactate/glucose rate ratios <2 this was indicative for an ongoing oxidative metabolism. Apart from this, M units demonstrated an elevated anaerobic glycolytic flux as evidenced by the increase in glucose consumption, lactate production and subsequent higher acidity according to previous reports on UV light-based PRTs [7,17,26,30,31,40]. Dekkers et al. also described a storage-related decline in pH accompanied by an increased glycolytic flux and suggested the pH decrease as the result rather than the cause of PSD [41].

Cellular demand for ATP is a driving force for regulation of energy delivery. Thus, alterations in PLT ATP consumption rate could explain why PLTs increased ATP producing processes after PRT treatment. As seen from the higher p selectin expression in stored M units, PRT treatment was associated with increased α granule degranulation. Secretion of intracellular PLT granules is an energy-dependent process and requires ATP [42]. Since mitochondria play a crucial role in energy delivery by oxidative phosphorylation, PRT treated PLTs might have up-regulated both mitochondrial function and glycolytic flux to counterbalance an increased ATP demand upon increased α granule degranulation. Furthermore, an increased ATP demand/consumption would disturb the ATP/ADP equilibrium between the mitochondrial and the cytosolic compartment and therefore probably explain the changes in the $\Delta\psi$ observed in stored M units relative to untreated/irradiated controls.

An unimpaired and even up-regulated respiratory function might be beneficial for PLT behaviour after transfusion in vivo. Here, clot retraction, a decisive marker for appropriate PLT function depends on sufficient ATP levels that, in fact, may profit from an ongoing oxidative metabolism. Furthermore, there is an abundance of data demonstrating the role of "oxygen burst" upon PLT activation [43–47]. PLT function inhibitors like ADP receptor antagonists were shown to impair mitochondrial metabolism, which emphasizes the critical role of intact mitochondrial activity for appropriate PLT function in vivo [48–50].

From the results of our study we conclude that Mirasol-PRT induced increase in glycolytic flux and mitochondria-based oxidative phosphorylation may be

Table 2
Blood gas and metabolic analysis of PLTs treated with Mirasol-PRT (M), 30 Gy gamma irradiation (X), or remaining untreated (C) throughout 7 days of storage.

Parameter	M = Mirasol-PRT treated (n = 12)				C = Untreated controls (n = 12)				X = Gamma irradiated (n = 12)			
	Day 0	Day 1	Day 5	Day 7	Day 0	Day 1	Day 5	Day 7	Day 0	Day 1	Day 5	Day 7
pH at 22 °C	7.33 ± 0.07[a,b]	7.41 ± 0.06[a,b]	6.97 ± 0.15[a,b]	6.50 ± 0.31[a,b]	7.25 ± 0.05[c]	7.52 ± 0.06[c]	7.43 ± 0.09[c]	7.29 ± 0.16[c]	7.25 ± 0.10[c]	7.53 ± 0.06[c]	7.41 ± 0.11[c]	7.27 ± 0.18[c]
pO_2 (mm Hg) at 22 °C	12.6 ± 3.6	16.9 ± 7.8	23.5 ± 5.0[a]	40.7 ± 24.8	13.3 ± 2.3	24.5 ± 11.3	33.3 ± 6.2[c]	40.6 ± 9.9	13.2 ± 4.1	24.7 ± 11.3	30.4 ± 6.9	41.1 ± 9.0
pCO_2 (mm Hg) at 22 °C	24.7 ± 3.7[a,b]	16.9 ± 2.8	12.7 ± 0.9	8.3 ± 1.9[a,b]	35.8 ± 4.2[c]	16.6 ± 2.3	11.9 ± 1.2	10.4 ± 0.8[c]	35.9 ± 7.1[c]	16.3 ± 2.2	12.3 ± 1.4	10.1 ± 0.9[c]
HCO_3^- (mmol/L)	15.4 ± 0.9[a,b]	12.7 ± 0.7[a,b]	3.9 ± 1.2[a,b]	1.2 ± 0.8[a,b]	18.9 ± 1.0[c]	15.6 ± 0.9[c]	9.3 ± 1.1[c]	6.3 ± 1.6[c]	18.8 ± 0.9[c]	15.6 ± 1.0[c]	9.2 ± 1.2[c]	6.0 ± 1.7[c]
Base excess (−mmol/L)	13.6 ± 1.5	14.0 ± 1.6[a,b]	30.1 ± 4.0[a,b]	41.8 ± 6.6[a,b]	12.5 ± 1.4	9.2 ± 2.6[c]	16.3 ± 2.8[c]	21.7 ± 4.5[c]	12.6 ± 2.2	9.3 ± 2.6[c]	16.7 ± 3.1[c]	22.2 ± 5.0[c]
LPR (nmoL/10^{12}cells/hr)		91 ± 46[a,b]	92 ± 24[a,b]	67 ± 16[a,b]		45 ± 29[c]	46 ± 16[c]	28 ± 6[c]		40 ± 27[c]	48 ± 16[c]	28 ± 9[c]
GCR (nmoL/10^{12}cells/hr)		43 ± 16[a,b]	63 ± 13[a,b]	71 ± 28[a,b]		20 ± 17[c]	31 ± 10[c]	36 ± 10[c]		17 ± 13[c]	32 ± 9[c]	40 ± 12[c]
OCR (nmoL/min/10^9 PLTs)	1.09 ± 0.14	1.09 ± 0.23[a,b]	0.94 ± 0.26[a,b]	0.57 ± 0.14	1.02 ± 0.10	0.77 ± 0.28[c]	0.58 ± 0.15[c]	0.47 ± 0.22	1.02 ± 0.12	0.75 ± 0.27[c]	0.66 ± 0.16[c]	0.45 ± 0.19

LPR lactate production rate. GCR glucose consumption rate. OCR oxygen consumption rate was calculated as = A × (130−pO_2) ÷ 760 ÷ C, where A is the oxygen transport rate (mL/m^2/day/atm) for the applied storage bag, and C the absolute total cell number. Significant compared to.

[a] Untreated units (C).
[b] Gamma irradiated units (X).
[c] PRT treated units (M).

the result of changes in the balance between ATP demand and supply, in favor of demand. According to prior authors [51], the question is whether additional components of the PLT storage medium such as acetate or amino acids may counterbalance the increased ATP demand after PRT treatment, thus reduce acceleration of PSD observed with these PLTs. Overall, the clinical significance of our findings for the behaviour of Mirasol-PRT treated PLTs in vivo remains to be evaluated in appropriate clinical trials. It was shown recently that plasma rescue to an optimal pH [52] or challenge with thrombin [53] improved morphology scores, stabilized osmotic recovery, and completely restored PLT secretory responses as measured by α granule release, with little change in the formation of apoptotic cells. Provided that PS exposure was not markedly enhanced, such PLTs had normal post-transfusion recoveries and survival rates [52].

Conflict of interest

All authors disclose any financial and personal relationships with other people or organizations that could inappropriately influence their work.

Acknowledgements

We would like to thank Inge Reynaerts (Navigant Biotechnologies, Lakewood, CO, USA) for kind assistance during data collection and Raymond P. Goodrich, Susanne Marschner (Navigant Biotechnologies) and Stef De Reys (Gambro BCT, Zeventem, Belgium) for excellent scientific support.

References

[1] Strammer SL, Glynn SA, Kleinman SH, Strong DM, Caglioti S, Wright DJ, et al. National heart, lung, and blood institute nucleic acid test study group. Detection of HIV-1 and HCV infections among antibody-negative blood donors by nuclei acid-amplification testing. National heart, lung, and blood institute nucleic acid test study group. N Eng J Med 2004;35:760–8.
[2] Li J, De Korte D, Woolum MD, Ruane PH, Keil SD, Lockerbie O, et al. Pathogen reduction of buffy-coat platelet concentrates using riboflavin and light: comparisons with pathogen reduction technology-treated apheresis platelet products. Vox Sang 2004;87:82–90.
[3] Goodrich L, Douglas I, Urioste M. Riboflavin photoinactivation procedure inactivates significant levels of bacteria and produces a culture negative product. Transfusion 2002;42:16S.
[4] Goodrich L, Ghielli M, Hansen E, Woolum M, Gampp D, Goodrich R, et al. Riboflavin and UV light inactivate enveloped and non-enveloped viruses in platelet concentrates under conditions, which maintain cell quality. Vox Sang 2002;83:111.
[5] Goodrich RP. Inactivation of viruses in blood products (platelets, plasma, and red cells). Transfus Clin Biol 2001;8:103S.
[6] Kumar V, Motheral T, Luzniak G, Goodrich RP. Mirasol pathogen reduction technology: riboflavin-based plasma process inactivates intracellular and extracellular human immunodeficiency virus. J Clin Apher 2003;18:84.
[7] Ruane PH, Edrich R, Gampp D, Keil SD, Leonard RL, Goodrich RP. Photochemical inactivation of selected viruses and bacteria in platelet concentrates using riboflavin and light. Transfusion 2004;44:877–85.
[8] Code of Federal Regulation, FDA, Vitamin B. CFR 21; Part 582.5695; 1998.
[9] Piper J, Hansen E, Woolum M. Evaluation of genotoxicity and acute toxicity risk associated with a riboflavin-based pathogen inactivation process. Int J Toxicol 2001;20:404.

[10] Zempleni J, Galloway JR, McCormick DB. Pharmacokinetics of orally and intravenously administered riboflavin in healthy humans. Am J Clin Nutr 1996;63:54–66.
[11] Unna K, Greslin J. Studies on the toxicity and pharmacology of riboflavin. J Pharmacol Exp Ther 1942;75:75–80.
[12] Joshi PC. Ultraviolet radiation-induced photodegradation and 1 O_2, O_2^- production by riboflavin, lumichrome and lumiflavin. Int J Biochem Biophys 1989;26:186.
[13] Kale H, Harikumar P, Nair PM, Netrawali MS. Assessment of the genotoxic potential of riboflavin and lumiflavin. Effect of metabolic enzymes. Mutat Res 1992;298:9–16.
[14] Hardwick CC, Herivel TR, Hernandez SC, Ruane PH, Goodrich RP. Separation, identification and quantification of riboflavin and its photoproducts using HPLC with fluorescence detection: a method to support pathogen reduction technology. Photochem Photobiol 2004;80:609–15.
[15] Akkerman JW. Regulation of carbohydrate metabolism in platelets: a review. Thromb Haemost 1978;39:12–24.
[16] Li J, Xia Y, Bertino AM, Coburn JP, Kuter DJ. The mechanism of apoptosis in human platelets during storage. Transfusion 2000;40:1320–9.
[17] Picker SM, Speer R, Gathof BS. Functional characteristics of buffy-coat PLTs photochemically treated with amotosalen-HCl for pathogen inactivation. Transfusion 2004;44:420–7.
[18] Snyder EL, Beardsley DS, Smith BR, Horne W, Johson R, Wooten T, et al. Storage of platelet concentrates after high-dose ultraviolet B irradiation. Transfusion 1991;31:491–6.
[19] Murphy S. Platelet storage for transfusion. Semin Hematol 1985;22:165–77.
[20] Li H, Zhu H, Xu CJ, Yuan J. Cleavage of BID by caspase 8 mediates the mitochondrial damage in the fas pathway of apoptosis. Cell 1998;94:491–501.
[21] Perrotta PL, Perrotta CL, Snyder EL. Apoptotic activity in stored human platelets. Transfusion 2003;43:526–35.
[22] Guidelines for the collection of blood and blood components and the usage of blood products (hemotherapy), Rev. ed. German Medical Association and Paul-Ehrlich-Institute. Cologne: Deutscher Ärzteverlag; 2005.
[23] Li J, Goodrich L, Hansen E, Edrich E, Gampp D, Goodrich RP. Platelet glycolytic flux increases stimulated by ultraviolet-induced stress is not the direct cause of platelet morphology and activation changes: possible implications for the role of glucose in platelet storage. Transfusion 2005;45:1750–8.
[24] Li J, Lockerbie O, De Korte D, Rice J, McLean R, Goodrich RP. Evaluation of platelet mitochondria integrity after treatment with Mirasol pathogen reduction technology. Transfusion 2005;45: 920–6.
[25] Perez-Pujol S, Tonda R, Lozano M, Fuste B, Lopez-Vilchez I, Galan AM, et al. Effects of a new pathogen reduction technology (Mirasol-PRT) on functional aspects of platelet concentrates. Transfusion 2005;45:911–9.
[26] Goodrich RP, Li J, Pieters H, Crookes R, Roodt J, Heyns AP. Correlation of in vitro platelet quality measurements with in vivo platelet viability in human subjects. Vox Sang 2006;90:279–85.
[27] Darzynkiewicz Z, Bedner E, Smolewski P. Flow cytometry in analysis of cell cycle and apoptosis. Seminars Hematol 2001;38:179–93.
[28] Verhoeven AJ, Verhaar R, Gouwerok EG, de Korte D. The mitochondrial membrane potential in human platelets: a sensitive parameter for platelet quality. Transfusion 2005;45:82–9.
[29] Kilkson H, Holme S, Murphy S. Platelet metabolism during storage of platelet concentrates at 22° C. Blood 1984;64:406–14.
[30] Janetzko K, Klinger M, Mayaudon V, Lin L, Eichler H, Klüter H. Storage characteristics of split double-dose platelet concentrates derived from apheresis and treated with amotosalen-HCl and UVA light for pathogen inactivation. Infus Ther Transfus Med 2002;29:193–8.
[31] Rhenen van DJ, Vermeij J, Mayaudon V, Hind C, Lin L, Corash L. Functional characteristics of S-59 photochemically treated platelet concentrates derived from buffy-coats. Vox Sang 2000;79:206–14.
[32] Snyder EL, Beardsley DS, Smith BR, Horne W, Johnson R, Wooten T, et al. Storage of platelet concentrates after high-dose ultraviolet B irradiation. Transfusion 1991;31:491–6.
[33] Mondoro TH, Shafer BC, Vostal JG. Restoration of in vitro responses in platelets stored in plasma. Am J Clin Pathol 1999;111:693–9.
[34] Bode AP. Platelet activation may explain the storage lesion in platelet concentrates. Blood Cells 1990;16:109–25.
[35] Seghatchian J. Platelet storage lesion: an update on the impact of various leukoreduction processes on the biological response modifiers. Transfus Apher Sci 2006;34:125–30.
[36] Shapira S, Friedman Z, Shapiro H, Presseizen K, Radnay J, Ellis MH. The effect of storage on the expression of platelet membrane phosphatidylserine and the subsequent impact on the coagulant function of stored platelets. Transfusion 2000;40:1257–63.
[37] Seghatchian J, Krailadsiri P. Platelet storage lesion and apoptosis: are they related? Transfus Apher Sci 2001;24:103–5.
[38] Leytin V, Freedman J. Platelet apoptosis in stored platelet concentrates and other models. Transfus Apher Sci 2003;28: 285–95.
[39] Xia Y, Li J, Bertino A, Kuter DJ. Thrombopoietin and the TPO receptor during platelet storage. Transfusion 2000;40:976–87.
[40] AuBuchon JP, Herschel L, Roger J, Taylor H, Whitley P, Li J, et al. Efficacy of apheresis platelets treated with riboflavin and ultraviolet light for pathogen reduction. Transfusion 2005;45:1335–41.
[41] Dekkers DW, De Cuyper IM, van der Meer PF, Verhoeven AJ, de Korte D. Influence of pH on stored human platelets. Transfusion 2007;47:1889–95.
[42] Gawaz MP. Blood platelets. New York: Georg Thieme Verlag Stuttgart; 2001.
[43] Muenzer J, Weinbach EC, Wolfe SM. Oxygen consumption of human blood platelets. Effect of inhibitors on thrombin-induced oxygen burst. Biochim Biophys Acta 1975;376:243–8.
[44] Kirtland SJ, Baum H. Mitochondrial respiration and the thrombin-induced release reaction of platelets. Biochem Pharmacol 1974;23:1859–70.
[45] Muenzer J, Weinbach EC, Wolfe SM. Oxygen consumption of human blood platelets. Effect of thrombin. Biochim Biophys Acta 1975;376:237–42.
[46] Pickett WC, Cohen P. Mechanism of the thrombin-mediated burst in oxygen consumption by human platelets. J Biol Chem 1976;251:2536–8.
[47] Mürer EH. Release reaction and energy metabolism in blood platelets with special reference to the burst in oxygen uptake. Biochim Biophys Acta 1968;162:320–6.
[48] Rognoni F, Viganò V, Colombo Pirola L. Influence of platelet anti-aggregants on mitochondrial respiration of platelets. Boll Soc Ital Cardiol 1977;22:2140–6.
[49] Abou-Khalil S, Abou-Khalil WH, Yunis AA. Mechanism of interaction of ticlopidine and its analogues with the energy-conserving mechanism in mitochondria. Biochem Pharmacol 1986;35:1855–9.
[50] Abou-Khalil WH, Lim LO, Yunis AA, Abou-Khalil S. Effects of ticlopidine, a new platelet antiaggregating agent, and its analogues on mitochondrial metabolism. Oxidative phosphorylation, protein synthesis and DNA polymerase activity. Biochem Pharmacol 1984;33:3893–8.
[51] Kaufman RM. Platelets: testing, dosing and the storage lesion-recent advances. Hematol Am Coc Hematol Educ Program 2006:492–6.
[52] Rinder HM, Snyder EL, Tracey JB, Dinecco D, Wang C, Baril L, et al. Reversibility of severe metabolic stress in stored platelets after in vitro plasma rescue or in vivo transfusion: restoration of secretory function and maintenance of platelet survival. Transfusion 2003;43:1230–7.
[53] Cavalho H, Alguero C, Santos M, de Sousa G, Trindada H, Seghatchian J. The combined effect of platelet storage media and intercept pathogen reduction technology on platelet activation/activability and cellular apoptosis/necrosis: Lisbon-RBS experience. Transfus Apher Sci 2006;34:187–92.

研究成果の刊行に関する一覧表

雑誌

発表者氏名	論文タイトル名	発表誌名	巻号	ページ	出版年
Noritaka Hashii, Nana Kawasaki, Satsuki Itoh, Yukari Nakajima, Akira Harazono, Toru Kawanishi, Teruhide Yamaguchi	Identification of glycoproteins carrying a target glycan-motif by liquid chromatography/multiple-stage mass spectrometry. Identification of Lewis x-glycoproteins in mouse kidney.	*J. Proteome Res.*	8	3415-3429	2009
Nana Kawasaki, Satsuki Itoh, Noritaka Hashii, Daisuke Takakura, Yuan Qin, Huang Xiaoyu, Teruhide Yamaguchi	The significance of glycosylation analysis in development of biopharmaceuticals.	*Biol. Pharm. Bull.*	32 (5)	796-800	2009
山口照英，石井明子	早期臨床開発段階でのバイオ医薬品の品質・安全性確保	臨床評価	36	611-627	2009

research articles Journal of proteome research

Identification of Glycoproteins Carrying a Target Glycan-Motif by Liquid Chromatography/Multiple-Stage Mass Spectrometry: Identification of Lewis x-Conjugated Glycoproteins in Mouse Kidney

Noritaka Hashii,[†,‡] Nana Kawasaki,[*,†,‡] Satsuki Itoh,[†] Yukari Nakajima,[†,‡] Akira Harazono,[†] Toru Kawanishi,[§] and Teruhide Yamaguchi[†]

Division of Biological Chemistry and Biologicals, National Institute of Health Sciences, 1-18-1 Kamiyouga, Setagaya-ku, Tokyo 158-8501, Japan, and Core Research for Evolutional Science and Technology (CREST) of the Japan Science and Technology Agency (JST), 4-1-8 Hon-cho, Kawaguchi, Saitama 332-0012 Japan

Received January 20, 2009

Certain glycan motifs in glycoproteins are involved in several biological events and diseases. To understand the roles of these motifs, a method is needed to identify the glycoproteins that carry them. We previously demonstrated that liquid chromatography−multiple-stage mass spectrometry (LC−MS^n) allowed for differentiation of oligosaccharides attached to Lewis-motifs, such as Lewis x (Le^x, Galβ1−4(Fucα1−3)GlcNAc) from other glycans. We successfully discriminated Le^x-conjugated oligosaccharides from other N-linked oligosaccharides derived from mouse kidney proteins by using Lewis-motif-distinctive ions, a deoxyhexose (dHex) + hexose (Hex) + *N*-acetylhexsosamine (HexNAc) fragment (*m/z* 512), and a Hex + HexNAc fragment (*m/z* 366). In the present study, we demonstrated that this method could be used to identify the Le^x-conjugated glycoproteins. All proteins in the mouse kidney were digested into peptides, and the fucosylated glycopeptides were enriched by lectin-affinity chromatography. The resulting fucosylated glycopeptides were subjected to two different runs of LC−MS^n using a Fourier- transform ion cyclotron resonance mass spectrometer (FTICR−MS) and an ion trap-type mass spectrometer. After the first run, we picked out product ion spectra of the expected Le^x-conjugated glycopeptides based on the presence of Lewis-motif-distinctive ions and assigned a peptide + HexNAc or peptide + (dHex)HexNAc fragment in each spectrum. Then the fucosylated glycopeptides were subjected to a second run in which the peptide-related fragments were set as precursor ions. We successfully identified γ-glutamyl transpeptidase 1 (γ-GTP1), low-density lipoprotein receptor-related protein 2 (LRP2), and a cubilin precursor as Le^x-conjugated glycoproteins by sequencing of 2−5 glycopeptides. In addition, it was deduced that cadherin 16, dipeptidase I, H-2 class I histocompatibility antigen, K−K alpha precursor (H2−K(k)), and alanyl (membrane) aminopeptidase could be Le^x-conjugated glycoproteins from the good agreement between the experimental and theoretical masses and fragment patterns. The results indicated that our method could be applicable for the identification and screening of glycoproteins carrying target glycan-motifs, such as Lewis epitopes.

Keywords: liquid chromatography/multiple-stage mass spectrometry • specific detection • database search analysis • Lewis x-conjugated oligosaccharides

Introduction

Glycosylation is one of the most common post-translational modifications of proteins.[1,2] Certain glycan motifs on glycoproteins are involved in several biological events, including cell adhesion,[3] differentiation and development. They are also known to be closely associated with some diseases, such as tumors and hepatic diseases.[4−6] Glycomics, the study of all glycoconjugates in a cell type or in an organism, is crucial to understanding the mechanisms of glycan-mediated biological events and diseases.[7,8] Mass spectrometry (MS) and multiple-stage mass spectrometry (MS^n) in combination with several types of chromatography are known to be the most powerful tools of structural glycomics.[9−14] There are two major approaches to mass spectrometric glycome analysis. One is mass spectrometric glycan profiling, which is achieved by online or off-line liquid chromatography/mass spectrometry (LC−MS) of oligosaccharides enzymatically or chemically released from proteins.[15−22] This technique has advantages for conducting a detailed structural analysis and a quantitative analysis of

* To whom correspondence should be addressed. Division of Biological Chemistry and Biologicals, National Institute of Health Sciences, 1-18-1 Kamiyouga, Setagaya-ku, Tokyo 158-8501, Japan. Fax: +81-3-3700-9084. E-mail: nana@nihs.go.jp.
† National Institute of Health Sciences.
‡ Japan Science and Technology Agency.
§ Division of Drugs, National Institute of Health Sciences.

10.1021/pr9000527 CCC: $40.75

oligosaccharides,[23−25] but it does not provide any information on protein sources that carry the glycans of interest. The other approach is the mass spectrometric mapping of proteolytic digests. This method enables us to characterize glycan structures based on fragment ions,[26−31] and to deduce the peptide sequence from b- and y-ions that arise from the peptide backbone.[27] In addition to these approaches, glycomics require more advanced methods that can identify target proteins carrying a glycan motif of interest; that is to say, a technique for focused glycomics.

Lectin and immunological-based approaches have been widely used for the specific detection of target glycans and glycoproteins.[32−34] There have been numerous reports on the use of MS in combination with affinity chromatography and Western blotting with lectins or glyco-epitope-specific antibodies.[35−38] In a previous study, we demonstrated that LC−MS^n is also useful for the analysis of target glycans in a complex mixture.[39] Several glycan motifs often yield motif-specific ions by MS^n, along with common glycan-related ions such as the *N*-acetylhexosamine (HexNAc) fragment (*m*/*z* 204) and hexose (Hex) + HexNAc fragment (*m*/*z* 366).[40,41] For example, Lewis-motifs that consist of fucose (Fuc), galactose (Gal) and *N*-acetylglucosamine (GlcNAc) yield a distinctive ion at *m*/*z* 512 that corresponds to the B-type ion of deoxyhexose (dHex) + Hex + HexNAc. This B-type ion subsequently provides the product ion at *m*/*z* 366 ([Hex + HexNAc]$^+$) by MS/MS/MS. Using these Lewis-motif-distinctive ions, we successfully differentiated the oligosaccharides bearing the Lewis-motifs from many other oligosaccharides in mouse kidneys.[39] This method could be used to differentiate the Lewis-conjugated glycopeptides from a proteolytic digestion of proteins. Furthermore, the protein sources of the Lewis-motif-conjugated glycopeptides could be identified by further MS^n of peptide-related ions.

In this study we demonstrated a method for the identification of Lewis x (Le^x, Galβ1−4(Fucα1−3)GlcNAc)-conjugated glycoproteins in tissue by LC−MS^n. Our method consists of two different runs of LC−MS^n using a Fourier-transform ion cyclotron resonance mass spectrometer (FTICR−MS) and ion trap-type mass spectrometer (IT-MS). After the first run, we sorted out the product ion spectra of expected Le^x-conjugated glycopeptides based on the presence of Lewis-motif-distinctive ions and assigned a peptide + HexNAc or peptide + (dHex-)HexNAc fragment in each spectrum. Then the fucosylated glycopeptides were subjected to a second run in which the peptide-related fragments were set as precursor ions (Figure 1). As a model tissue, we used a mouse kidney in which we previously confirmed the presence of the Galβ1−4(Fucα1−3)GlcNAc motif (Lewis x and y) as well as the absence of the Galβ1−3(Fucα1−4)GlcNAc motif (Lewis a and b) and Fucα1−2Galβ1−3/4GlcNAc motif (blood group H).[39]

Experimental Section

Materials. Trypsin (Trypsin Gold, mass spectrometry grade), *Aleuria aurantia* lectin (AAL)-immobilized agarose column and Peptide-*N*-glycosidase F (PNGase F) were purchased from Promega (Madison, WI), Honen (Tokyo, Japan) and Roche (Mannheim, Germany), respectively. Murine kidneys (MRL/MpJ-lpr/lpr) were purchased from Japan SLC Inc. (Hamamatsu, Japan).

Sample Preparation. Murine kidney cells were filtrated by a cell strainer (70 μm; BD Biosciences, San Jose, CA) and solubilized in lysis buffer (7 M urea, 2 M thiourea, 2% CHAPS, and 30 mM Tris-HCl) containing a protease inhibitor mixture (Wako, Tokyo, Japan) by vortexing at 4 °C. After quantifying the proteins, cold acetone (final concentration, 80%(v/v)) was added to the protein solution (500 μg protein). The precipitated protein was dissolved again in 100 μL of 0.5 M Tris-HCl, pH 7.0, and precipitated with an 8-fold volume of acetone. The precipitated protein was dissolved in 810 μL of 0.5 M Tris-HCl (pH 8.6) containing 8 M guanidine-HCl and 5 mM EDTA, and the mixture was incubated with 6.0 μL of 2-mercaptoethanol at room temperature for 2 h. Freshly prepared 0.6 M sodium monoiodoacetate (135 μL) was added to the solution, and the mixture was incubated at room temperature for 2 h in the dark. The reaction mixture was desalted with a PD10 column (GE Healthcare Bio-Sciences, Uppsala, Sweden), and the solution containing proteins was freeze-dried. The carboxymethylated proteins were dissolved in 500 μL of bicarbonate buffer (pH 8.5) and incubated with 2 μg of trypsin at 37 °C for 16 h. After deactivation of trypsin by boiling for 3 min, a 10-fold volume of phosphate buffered saline (PBS) was added to the reaction mixture.

Lectin Affinity Chromatography. The sample solution was applied to the AAL-immobilized agarose column (1.45 mg of lectin, 1.5 × 1.0 cm) and washed with 2.5 mL of cold PBS at 4 °C (approximately one drop/s). The absorbed glycopeptides were eluted with PBS containing 0.2 M fucose (2.5 mL), and the fraction was desalted with a C18 cartridge (Micro Trap, 8.0 × 1.0 mm; Michrom BioResources, Auburn, CA). The absorbed glycopeptides in the cartridge were eluted with 2 mL of 0.1% trifluoroacetic acid containing 45% acetonitrile, and the fraction was dried, resuspended in 0.1% formic acid, and then analyzed by LC−MS^n.

PNGase F Treatment. Fucosylated glycopeptides enriched by lectin affinity chromatography were treated with 10 units of PNGase F in 50 μL of 50 mM phosphate buffer (pH 8.0) at 37 °C for 48 h to release *N*-linked oligosaccharides. After terminating the reaction by boiling, the reaction mixture was evaporated to dryness, resuspended in 0.1% formic acid, and then analyzed by LC−MS/MS.

Online Liquid Chromatography/Mass Spectrometry (LC−MS). Chromatographic separation of the fucosylated glycopeptide was performed using the Paradigm MS4 HPLC system (Michrom BioResources). The fucosylated glycopeptides were dissolved in 25 μL of 0.1% formic acid, and 2 μL of the sample solution was injected into 2 μL capillary loop. The analytical column was a reversed-phase capillary column (Magic C18, 50 × 0.2 mm, 5 μm; Michrom BioResources). The mobile phase was 0.1% formic acid containing 2% acetonitrile (A buffer) and 0.1% formic acid containing 90% acetonitrile (B buffer). The fucosylated glycopeptides were eluted at a flow rate of 2 μL/min with a gradient of 5−65% of B buffer in 90 min.

Mass spectrometric analysis of fucosylated glycopeptides was performed using a FTICR/IT−MS (LTQ-FT; Thermo Fisher Scientific, Waltham, MA) equipped with a nanoelectrospray ion source (AMR, Tokyo, Japan). The conditions for FTICR−MS and IT−MS were as follows: an electrospray voltage of 2.0 kV in positive ion mode, a capillary temperature of 200 °C, a tube lens offset of 140 V, a collision energy of 35% for the MS^n experiment, maximum injection times (FTICR−MS and IT−MS) of 1250 and 50 ms, respectively, a resolution of FTICR−MS of 50 000, a scan time of approximately 0.2 s, dynamic exclusion of 18 s, and an isolation width of 3.0 u (range of precursor ion ±1.5).

First Run. The mass spectrometric mapping of fucosylated glycopeptides was performed by a sequential scan: full mass scan using FTICR−MS (*m*/*z* 1000−2000), data-dependent

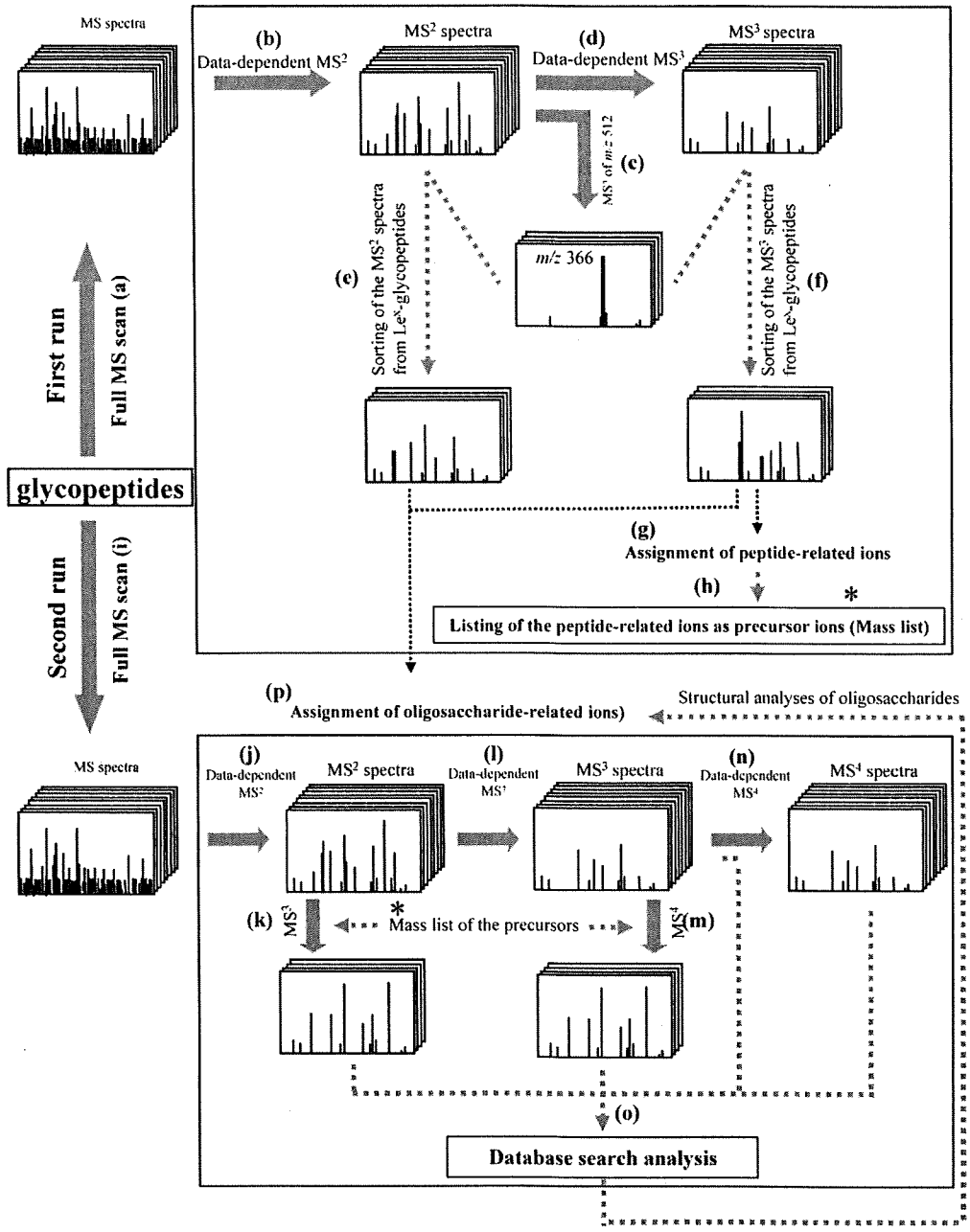

Figure 1. Strategy for the identification of Le^x-conjugated glycopeptides by LC–MS. The fucosylated glycopeptides were subjected to two different runs. In the first run, fucosylated glycopeptides were analyzed by (a) a full mass scan using the FTICR–MS, (b) data-dependent MS/MS, (c) MS/MS/MS of the Le^x-motif-distinctive ion (m/z 512), and (d) data-dependent MS/MS/MS. (e, f) On the basis of the presence of the product ion at m/z 512, which subsequently yielded the ion at m/z 366 by the MS/MS/MS, MS/MS and MS/MS/MS spectra of Le^x-conjugated glycopeptides were picked out from all the acquisition data. (g) Peptide-related ions were ascertained in the MS/MS/MS spectra. (h) The peptide-related ions were listed as precursor ions. In the second run, the fucosylated glycopeptides were identified by a full MS scan using the (i) FTICR-MS, (j) data-dependent MS/MS, (k) MS/MS/MS of the peptide-related ions listed as precursor ions, (l) data-dependent MS/MS/MS, (m) MS/MS/MS/MS of the peptide-related ions, and (n) data-dependent MS/MS/MS/MS. (o) Product ion spectra were submitted to database search analysis with a static modification of Cys with carboxymethyl (58.0 u) and possible modification of Asn with HexNAc (203.1 u) and dHex + HexNAc (349.1 u). MS^2, MS/MS; MS^3, MS/MS/MS; MS^4, MS/MS/MS/MS. (p) Carbohydrate structures were deduced from the oligosaccharide-related ions in the MS/MS and MS/MS/MS spectra.

MS/MS, MS/MS/MS of the Le^x-motif-distinctive ion (m/z 512) generated in data-dependent MS/MS, and MS/MS/MS of the most intense ions generated in data-dependent MS/MS by MS^n using IT–MS. Based on the presence of the product ion at m/z 512 that subsequently yielded the ion at m/z 366 by the MS/MS/MS, the MS/MS and MS/MS/MS spectra of expected Le^x-conjugated glycopeptides were picked out from all the acquisition data. Peptide-related ions were ascertained in the MS/MS/MS spectra, and were listed as precursor ions for the second run.

Second Run. Peptide sequencing was performed in a sequential scan: a full mass scan using FTICR−MS (*m/z* 1000−2000), data-dependent MS/MS, MS/MS/MS of the peptide-related ions listed as precursor ions, data-dependent MS/MS/MS, MS/MS/MS/MS of the peptide-related ions, and data-dependent MS/MS/MS/MS using IT−MS.

Protein Identification by Database Search Analysis. The spectra data obtained by the data-dependent collision-induced dissociation (CID)s and predominant CIDs of peptide-related ions were subjected to database search analysis with the TurboSEQUEST algorithm (BioWorks 3.1; Thermo Fisher Scientific) by using the NCBInr database (*Mus musculus*, 28−11−06). The static modification of carboxymethylation (58.0 u) at Cys, and the possible modification of HexNAc (203.1 u) and dHex + HexNAc (349.1 u) at Asn were used as the modified parameters of database search analysis. The SEQUEST criteria, known as cross correlation (Xcorr) scores, were set to 1.5/2.0/2.5 (charge states of +1/+2/+3) for the protein identifications. DTA files were generated for spectra with a threshold of 10 ions and a TIC of 100. Precursor and fragment ion mass tolerance in the MS^n spectra for database search analysis were set to 2.0 u and 1.0 u, respectively.

Results

Sorting out the Product Ion Spectra of the Le^x-Conjugated Glycopeptides by the First LC−MS/MS/MS Run. Proteins from mouse kidney cells were carboxymethylated and digested with trypsin. In the mass spectrometric mapping of the proteolytic digest, we often fail to acquire glycopeptide ions due to their lower ionization efficacy compared to coeluted unmodified peptides. To prevent interference by peptides in the ionization of glycopeptides, fucosylated glycopeptides including Lewis-motif-conjugated glycopeptides were enriched by affinity chromatography with an AAL-immobilized agarose column. The fucosylated glycopeptides were desalted by a C18 cartridge and injected into an LC−MS system equipped with FTICR−MS for a MS scan (*m/z* 1000−2000). The most intense ions on the MS scan were subjected to data-dependent MS/MS and MS/MS/MS, and an additional MS/MS/MS was performed when a dHex + Hex + HexNAc fragment (*m/z* 512) was detected on the MS/MS scan (Figure 1, first run). Figure 2A, B and C show the total ion chromatograms (TIC) obtained by the FTICR−MS scan of the fucosylated glycopeptides, the extracted ion chromatogram (EIC) of the dHex + Hex + HexNAc fragment acquired on the data-dependent MS/MS scan, and the EIC of the Hex + HexNAc fragment (*m/z* 366) that arose from the fragment at *m/z* 512 by the MS/MS/MS, respectively. We presumed that the Le^x-conjugated glycopeptides had been eluted around the peaks appearing in Figure 2C.

Assignments of the Peptide-Related Ions Derived from the Expected Le^x-Conjugated Glycopeptides. We picked out dozens of product ion spectra, and 22 precursors were determined to be the Le^x-conjugated glycopeptide-derived mass spectra based on the presence of Le^x-motif-distinctive ions. The elution positions of the glycopeptides are indicated in Figure 2C. In our previous report, most of the *N*-glycosylated peptides yielded peptide-related ions, such as $[\text{peptide} + \text{HexNAc} + \text{nH}]^{(n-1)+}$ and $[\text{peptide} + (\text{dHex})\text{HexNAc} + \text{nH}]^{n+}$, which provided peptide fragment b- and y-ions by further CID, and subsequent database search analysis successfully revealed the peptide sequences of the glycopeptides.[27] In the present study, therefore, we examined the peptide-related ions in the product ion spectra of the glycopeptides 1−22 for peptide sequencing.

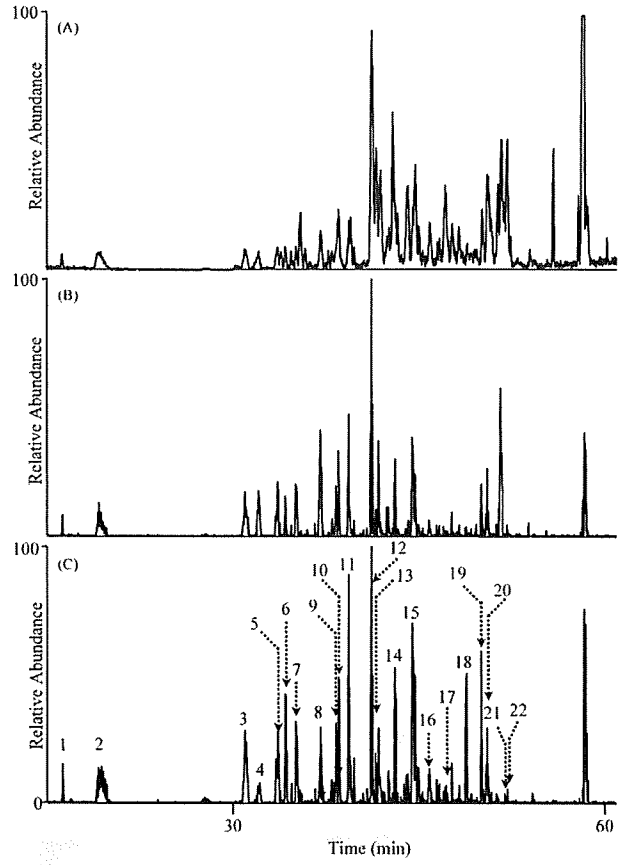

Figure 2. LC−MS^n of fucosylated glycopeptides. (A) Total ion chromatogram (TIC, *m/z* 1000−2000) of fucosylated glycopeptides. (B) Extracted ion chromatogram (EIC) of the ion at *m/z* 512 produced by data-dependent MS/MS. (C) EIC of the product ions at *m/z* 366 produced from the product ion at *m/z* 512 by MS/MS/MS. Expected Le^x-conjugated glycopeptides were designated as glycopeptides 1−22.

Figure 3A shows the integrated mass spectrum of the expected Le^x-glycopeptides eluted at 41−43 min. On the basis of an *m/z* spacing pattern that included *m/z* 67.69 ($HexNAc^{3+}$), *m/z* 54.02 (Hex^{3+}) and 48.69 ($dHex^{3+}$), intense ions at *m/z* 1067.105, 1134.803, 1189.505, and 1237.508 were assigned to triply charged ions of glycopeptides differing in glycosylation. Two intense ions, glycopeptides 12 (*m/z* 1237.508) and 13 (*m/z* 1134.803), were further subjected to MS/MS and MS/MS/MS, and yielded identical peptide-related ions at *m/z* 1650 (Figure 3B, C). This result indicates that glycopeptides 12 and 13 are glycoforms containing Le^x-motifs, and implies that the carbohydrate heterogeneity of a peptide of interest could be deduced from the integrated mass spectra.

Figure 4A indicates the MS/MS spectrum of glycopeptide 8. The presence of a dHex + Hex + HexNAc fragment (*m/z* 512) suggests that this glycopeptide is one of the Le^x-conjugated glycopeptides. The most intense fragment (*m/z* 1681.0) was further subjected to MS/MS/MS and provided a series of doubly charged Y-ions with an *m/z* spacing pattern, including *m/z* 101 ($HexNAc^{2+}$) and *m/z* 81 (Hex^{2+}). It was revealed that the fragment at *m/z* 906.2 was our desired product ion, $[\text{peptide} + \text{HexNAc} + 2\text{H}]^{2+}$ (Figure 4B).

Figure 5A and B show the MS/MS and MS/MS/MS spectra of glycopeptide 15, respectively. The triply charged ion (*m/z* 1414.4)

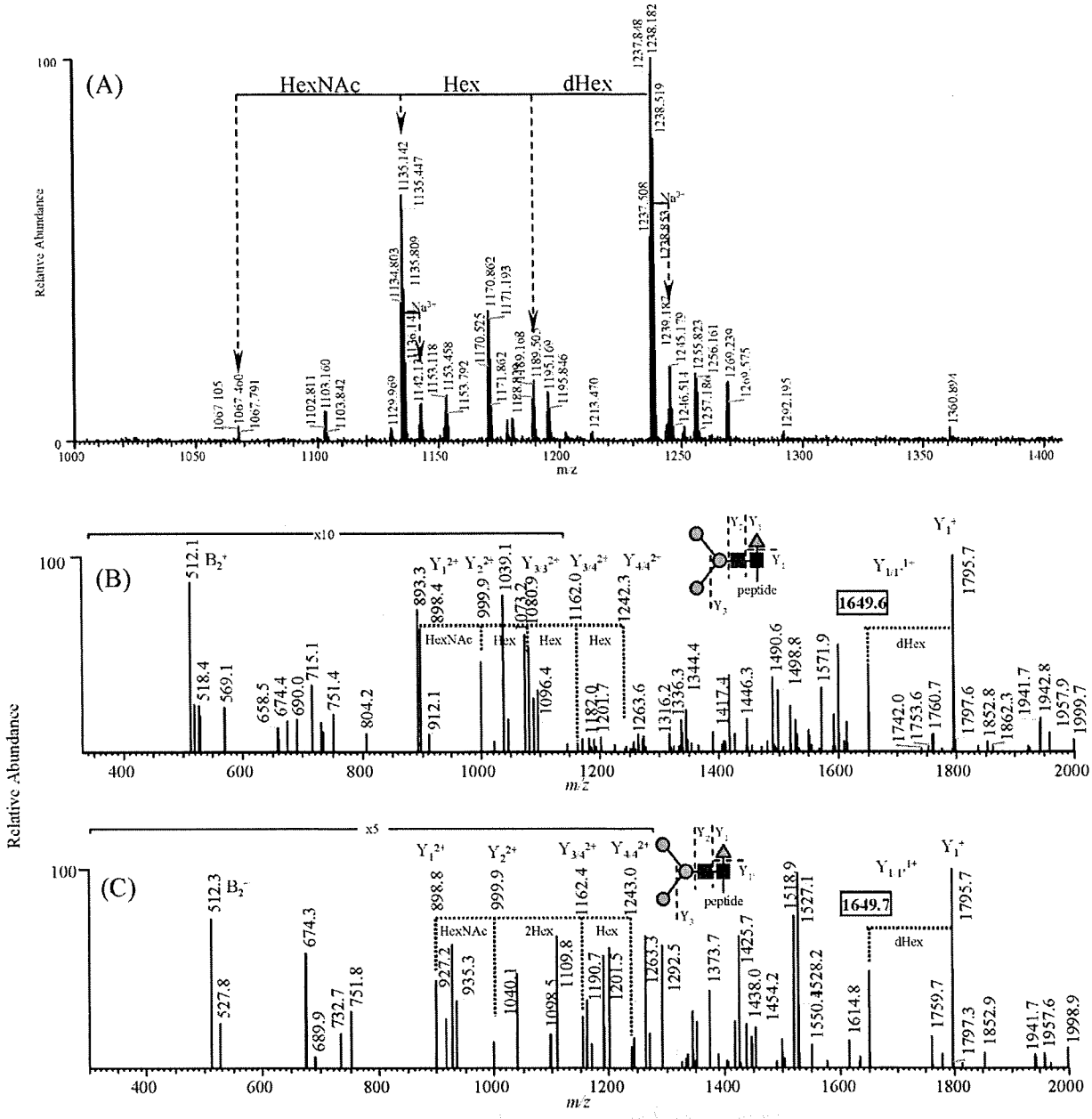

Figure 3. Integrated mass spectrum and MS/MS/MS spectra of glycopeptides 12 and 13. (A) Integrated mass spectrum of the expected Le^x-glycopeptides eluted at 41−43 min. (B) MS/MS/MS spectrum acquired from the most intense ion (*m/z* 1673.4) detected in the MS/MS spectrum of glycopeptide 12 (*m/z* 1237.8). (C) MS/MS/MS spectrum acquired from the most intense ion (*m/z* 1601.0) detected in the MS/MS spectrum of glycopeptide 13 (*m/z* 1135.4).

on the MS/MS scan was further subjected to MS/MS/MS and yielded a Y-ion series that included [peptide + 2HexNAc + 3Hex + dHex + 2H]$^{2+}$ (*m/z* 1764.3), [peptide + 2HexNAc + 2Hex + dHex+ 2H]$^{2+}$ (*m/z* 1683.5), [peptide + 2HexNAc + dHex + 2H]$^{2+}$ (*m/z* 1520.2), and [peptide + 2HexNAc + 2H]$^{2+}$ (*m/z* 1447.0). The fragment detected at *m/z* 1346.3 was assigned to our target ion, [peptide + HexNAc + 2H]$^{2+}$.

Alternative MS/MS and MS/MS/MS spectra of a Le^x-conjugated glycopeptide (glycopeptide 17) are shown in Figure 6A and B, respectively. The fragment at *m/z* 1515.4 on the MS/MS scan yielded Y-ion series that included [peptide + 2HexNAc + 3Hex + 2H]$^{2+}$ (*m/z* 1659.6), [peptide + 2HexNAc + 2Hex + 2H]$^{2+}$ (*m/z* 1578.3), and [peptide + 2HexNAc + 2H]$^{2+}$ (*m/z* 1416.5) on the MS/MS/MS scan. We deduced that the fragment at 1315.0 on the MS/MS/MS scan could be [peptide + HexNAc + 2H]$^{2+}$.

Finally we assigned out peptide + HexNAc, peptide + (dHex)HexNAc, and the peptide fragment from the product ion spectra of Le^x-conjugated glycopeptides 1−22 (Table 1). These peptide-related ions were listed as precursor ions in the second run, in which the listed ions were predominantly submitted to CID (Figure 1, second run).

Peptide Sequencing of the Expected Le^x-Conjugated Glycopeptides by the Second LC−MS/MS/MS/MS Run and Database Search Analysis. In the second run and subsequent database search analysis with modified parameters, including